UNIVERSITI MALAYSIA PAHANG

DECLARATION OF THESIS AND COPYRIGHT

Author's Full Name : YONG ZONG WEI

Date of Birth : 10.4.1993

Title : AUTONOMOUS MOBILE ROBOT USING MYRIO

Academic Session : 2016/2017

I declare that this thesis is classified as:

☐	CONFIDENTIAL	(Contains confidential information under the Official Secret Act 1997)*
☐	RESTRICTED	(Contains restricted information as specified by the organization where research was done)*
☑	OPEN ACCESS	I agree that my thesis to be published as online open access (Full Text)

I acknowledge that Universiti Malaysia Pahang reserves the following rights:

1. The Thesis is the Property of Universiti Malaysia Pahang
2. The Library of Universiti Malaysia Pahang has the right to make copies of the thesis for the purpose of research only.
3. The Library has the right to make copies of the thesis for academic exchange.

Certified by:

(Student's Signature)

YONG ZONG WEI
930410-05-5209
Date: 8 JUNE 2017

(Supervisor's Signature)

1. EN.ISMAIL BIN MOHD KHAIRUDDIN
2. DR. AHMAD SHAHRIZAN BIN ABDUL GHAN

Date: 8 JUNE 2017

REPORT DECLARATION LETTER (OPTIONAL)

Librarian,
Perpustakaan Universiti Malaysia Pahang,
Universiti Malaysia Pahang,
Lebuhraya Tun Razak,
26300, Gambang, Kuantan.

Dear Sir,

CLASSIFICATION OF THESIS AS RESTRICTED

Please be informed that the following thesis is classified as RESTRICTED for a period of three (3) years from the date of this letter. The reasons for this classification are as listed below.

Author's Name
Thesis Title

Reasons (i)

(ii)

(iii)

Thank you.

Yours faithfully,

____
(Supervisor's Signature)

Date:

Stamp:

SUPERVISOR'S DECLARATION

We hereby declare that we have checked this report and in my opinion, this report is adequate in terms of scope and quality for the award of the degree of Bachelor of Engineering in Mechatronics.

(Supervisor's Signature)

Full Name : EN.ISMAIL BIN MOHD KHAIRUDDIN

Position :

Date :

(Co-supervisor's Signature)

Full Name : DR. AHMAD SHAHRIZAN BIN ABDUL GHANI

Position : Lecturer

Date : 8 JUNE 2017

Universiti Malaysia PAHANG
Engineering • Technology • Creativity

STUDENT'S DECLARATION

I hereby declare that the work in this report is based on my original work except for quotations and citations which have been duly acknowledged. I also declare that it has not been previously or concurrently submitted for any other degree at Universiti Malaysia Pahang or any other institutions.

(Student's Signature)

Full Name : YONG ZONG WEI

ID Number : FB13053

Date : 8 JUNE 2017

USING MYRIO

YONG ZONG WEI

Report submitted in partial fulfillment of the requirements
for the award of the degree of
Bachelor of Engineering (Hons.) Mechatronic Engineering

Faculty of Manufacturing Engineering

UNIVERSITI MALAYSIA PAHANG

JUNE 2017

ACKNOWLEDGEMENTS

First and foremost, I would like to thanks to god for providing me strength and blessings to complete this thesis and finish my project on time. This project would not be able to complete if without any help for the people around me.

Next, I am grateful and would like to express my sincere gratitude to my supervisors En.Ismail Bin Mohd Khairuddin and Dr. Ahmad Shahrizan Bin Abdul Ghani for providing me an opportunity to work with them. Without their germinal and helpful idea yet offered an invaluable assistance, this project will not be able to successful complete. Besides, they had always impressed me with their professional conduct their strong conviction for success.

Other than that, I would like to thank all my friend who helped me in this project. They provided me very useful idea and help me whenever I am facing trouble and giving me moral support.

Last but not least, a special thanks to my parents for the moral support and some financial support to help me throughout this project. Their endless love give me a lot of energy to complete my thesis.

ABSTRAK

Kajian penyelidikan menunjukan robot mudah alih autonomi dan banyak kajian dijalankan untuk mengurangkan kerja-kerja manusia dan memudahkan kerja. Dalam penyelidikan, robot mudah alih amat berguna untuk manusia kerana bahaya dan batasan manusia mempunyai sebab utama keperluan untuk robot mudah alih yang lebih serba boleh dan berkuasa, terutamanya dalam industri pemesinan dan pengkalan tentera. Selain itu, reka bentuk yang stabil untuk robot mudah alih boleh mudah untuk bergerak dalam alam sekitar. Selain itu, navigasi dan halangan objek juga digunakan peguam dalam robot mudah alih. Dalam projek ini, kajian penyelidikan yang dijalankan untuk membangunkan algoritma robot mudah alih autonomi dengan pelaksanaan pemodelan dinamik menggunakan Newton-Euler approach.The jasad tegar daripada robot mudah alih dilengkapi dengan dua roda dan kastor untuk tujuan kawalan mudah dan stabil mengimbangi. Di samping itu, Kinect sensor gerakan akan digunakan untuk mengesan imej dan rakaman video semasa sensor ultrasonik mengelakkan halangan daripada robot mudah alih. Sebaliknya, simulasi mekanisme kawalan direalisasikan melalui pakej perisian LabVIEW mana pembangunan persekitaran robot mudah alih dijalankan dan dipindahkan ke perkakasan Instrumen Nasional Myrio. Keputusan mendapati bahawa robot mudah alih autonomi berjaya halangan dan merakam video semasa menggunakan kedua-dua sensor. Adalah dipercayai bahawa robot mudah alih ini boleh digunakan dalam persekitaran bahaya untuk merekodkan semua data penting yang memerlukan persekitaran mereka.

ABSTRACT

Current research show that autonomous mobile robot is being widely researched to reduce human work and ease the job. In the research, mobile robot very useful for human because hazards and human limitations have the main reason for the need for more versatile and powerful mobile robots, especially in machining industry and military bases. Besides that, stable design for mobile robot can easy to move in any environmental. Moreover, the navigation and obstacle the object also famous used in mobile robot. In this project, the research study is conducted to develop an autonomous mobile robot algorithm with implementation of dynamic modelling using Newton-Euler approach.The rigid body of the mobile robot is equipped with two wheels and a castor for the purpose of simple control and stable balancing. In addition, Kinect motion sensor will be applied for the image detection and video recording while ultrasonic sensor obstacle avoidance of the mobile robot. On the other hand, the simulation of the control mechanism is realized through LabVIEW software package where the development of the mobile robot environment is carried out and transferred to National Instrument myRIO hardware. Results found that the autonomous mobile robot successfully obstacle and record video while using both sensors. It is believed that this mobile robot can used in hazards environment to record all the important data that need those environment.

TABLE OF CONTENT

LIST OF TABLES

LIST OF FIGURES

LIST OF SYMBOLS

K_p	Proportional gain
K_i	Integral gain
K_d	Derivative gain
θ	Heading/ angle
X	Speed in x direction
ω	Angular velocity
Y	Speed in y direction
R	[Ω] resistance of the motor winding
L	[H] inductance of the motor
K	[kg.m2. s-2. A-1] electromotive constant
U_0	[V] voltage of the source
Ω	[rad. s-1] angular velocity of the rotor
i	[A] current flow in the winding
J	[kg.m2] moment of inertia
k_r	[kg.m2. s-1] resistance coefficient of rotation
M_x	[kg.m2. s-2] moment of the load
m	[kg] mass of the robot
k_v	[kg. s-1] linear motion's resistance coefficient
M_{GL}	[kg.m2. s-2] left drive's moment
M_{GP}	[kg.m2. s-2] right drive's moment
v_B	[m.s-1] speed of linear motion
r	[m] Wheel's semi-diameter.
l_P	[m] distance between point B and right wheel,
l_L	[m] distance between point B and left wheel,
l_T	[m] distance between centre of gravity and point B,
k_ω	[kg.m2. s-1] rotary motion's resistance coefficients
J_T	[kg.m2] MoI with respect to rotation axis in centre of gravity
ω_B	[s-1] angular speed in point B.
l_P	[m] distance between point B and right wheel,

LIST OF ABBREVIATIONS

WMR	Wheeled Mobile Robot
SoC	System on Chip
I/O	Input and Output
IR	Infrared
PID	Proportional-Integral-Derivation
SLAM	Simultaneous Localization And Mapping
MoI	Moment of Inertia
CMOS	Complementary Metal-Oxide- Semiconductor

CHAPTER 1

INTRODUCTION

This chapter mainly focuses on the general idea of this study along the project background, problem statement, project objectives and scope that covered on this project.

1.1 Background Study

Robotics had subdivided off the science that includes electrical engineering, manufacturing engineering, mechatronics engineering and others. As we know, robotics had attained a greatest successful in industrials on this world. There are many types of industrial applications using robotics such as the robot arm, mobile robots and other. The most popular robotics on this world is mobile robots. The hardware and software of mobile robot has been designed for the purpose of extreme environment, such that it will be able to perform their tasks in the presence of noise. In some cases where dynamic environment is involved, the mobile robot could not be able to perform good task such that the feedback from the robot is contradictory to the current situation being measured and inconsistent response information for a continuously changing environment.(Ali, 2011). Nowadays, mobile robots have been evolving to move automatically from one places to other locations. For daily activities, mobile robots have been extensively developed and researched to assist humans for doing daily activities. Mobile robots is widely developed to reduce human work and easy the job. In this situation, mobile robots can expand work to convey an expanding inclination for mechanical fabricating exercise. Typically, the above-described mobile robots will used in industrials.

However, due to extensive research in mobile robot. There are a lot of application of mobile robots for nowadays. Every situation in which an animal, human or vehicle involves in a useful work today provides a potential application for a mobile robot. Based on reports, by implementing mobile robot in industrial manufactures can improve product quality, reduce overheads, increase rates of production and so on. Mobile robots types and application will show at the figure below.

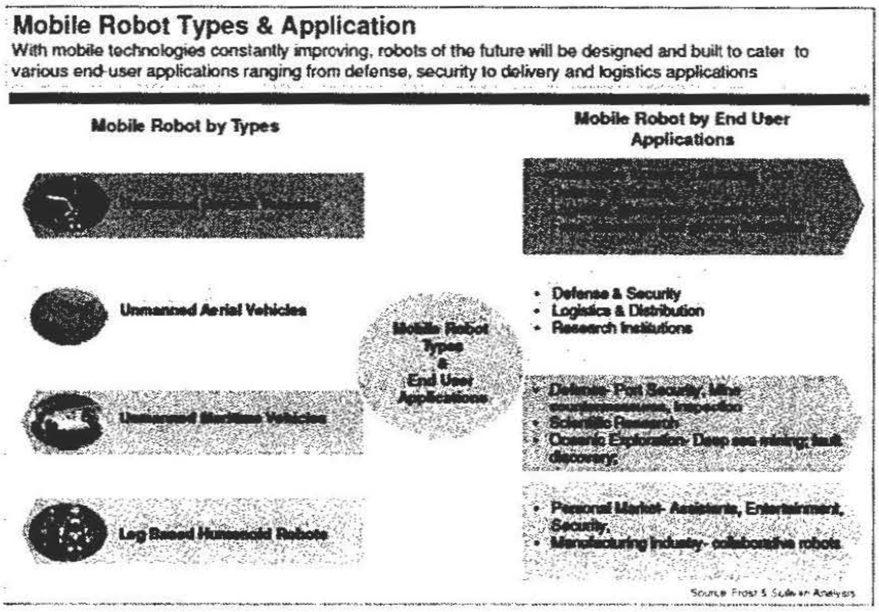

Figure 1.1 Mobile robot types and application.
Source: Frost & Sullivan Analysis, 2014

The widely used type of mobile robots are wheeled mobile robot also can name as WMR. WMR are most popular in mobile robots because WMR is using differential-drive system and it also alternative in simply design and manoeuvrable. Simple explanation for WMR are combination with computational (software) and various physical (hardware) components. In subsystems of WMR are locomotion, sensing, communication, reasoning and control. Each subsystems will apply in WMR.

WMR does not only depend on the tracking system, the control and drive system also necessary. For the control algorithm, it made up with the mathematical model properties in WMR. The mathematical model for WMR can explain in two ways, which are dynamics and kinematic models. Commonly dynamic modelling will be omitted when developing in mathematical models of WMR (Shojaei, Mohammad Shahri, & Tarakameh, 2011). While both modelling are the preferred system accuracy.

Apart from that, navigation mobile robots also famous and widely in the field of robotics. Navigation can be combination of the self –localisation, path planning and map-building competence (Becerra, Courbon, Mezouar, & Sagues, 2010). National Instruments myRIO (NI myRIO) is an embedded hardware device. It can prove technology and allows to complex engineering systems more quickly, design real and affordably than ever before. NI myRIO can incorporate the interfacing and advantages for programming in LabVIEW (White, Wagner, Blankenau, Wang, & Salazar, 2015).

In this project, the mobile robot is considered as autonomous, if it has a few capabilities. Mobile robot should be able to locate at indoor environment. Lastly, mobile robot should be detect navigate an environment with obstacles while using ultrasonic and Kinect sensor as image capture.

1.2 Problem Statement

Nowadays, service applications using autonomous mobile robot have been considered such as intelligent wheelchair, food delivery and vacuum cleaners mobile robot. For those robots, it must recognize a specific object and it can be required to relocate and approach. The navigation can used in a mobile robot to develop a control system. An optimal navigation system that enables the mobile robot to move in entire area. The choice of vision based object recognition technique for mobile robot have some difficulties such as direction of the mobile robot to move and relocation as required that will involves selecting vision sensor's viewpoint. The most challenging problem is the object detection process because mobile robot need to navigate and place the object in view field. Besides that, the mobile robot also required a vision system that can use in object detection process. The mobile robot can aware to start and target location through the path planning process. While in target position for mobile robot is unknown. Therefore the path should be cover the entire area and maximise the probability for detect the object.

1.3 Project Objective

The objectives of this project are as below:

1. To design a robot with mobility in indoor environment.
2. To accomplish object avoidance using ultrasonic sensor while Kinect sensor as image capturing device
3. To develop LabVIEW simulation for the robot's control.

1.4 Project Scope

The purpose of scope for this project is limited to:

1. Use Kinect sensor and ultrasonic sensors to capture image and avoid obstacles respectively.
2. Autonomous mobile robot is used in indoor environmental.
3. The PID control algorithm is implemented to control the mobile robot moving with high accuracy.
4. Implementing NI myRIO device as the microcontroller to control the mobile robot.

CHAPTER 2

LITERATURE REVIEW

2.1 Introduction

For each research project it is required to comprehensive review of the accumulated knowledge in the field. This chapter will discuss methodologies, sensor technologies and mathematical modelling methods applied provides researches.

2.2 Design and Develop an Autonomous Mobile Robot

The suitable base is vital to develop a fully functional mobile robot. Normally, base of mobile robot is determines from the kinematic equation for control the motion of the mobile robot. So, there are a lot of difference base in mobile robot design. While in the motion of mobile robot can be classified into two categories which are wheeled and legged. In this project for autonomous mobile robot will focus on wheeled robot and this is commonly use in design project. WMR is efficient and apply a simple mechanical system. In design and development of an autonomous mobile robot a few aspects need to be considered base on the types of base and wheel.

2.2.1 Wheeled Mobile Robot (WMR)

WMR always designed for their wheels are in the ground contact for all the times. Usually research for WMR that need to focus on those problem are traction and stable, manoeuvrability and control. Four type of basic wheel classes (Ali, 2011), as shown in Figure 2.1;

a. Standard wheel with two degrees of freedom (rotation around the motorised axle, rotation around the touch point).

b. Two degrees of freedom for castor wheel (rotation surrounding the offset steering joint and the touch point).
c. Three degrees of freedom for Swedish wheel (rotation surrounding the motorised wheel axle, rollers, and touch point).
d. Spherical or ball wheel that can spin along any direction.

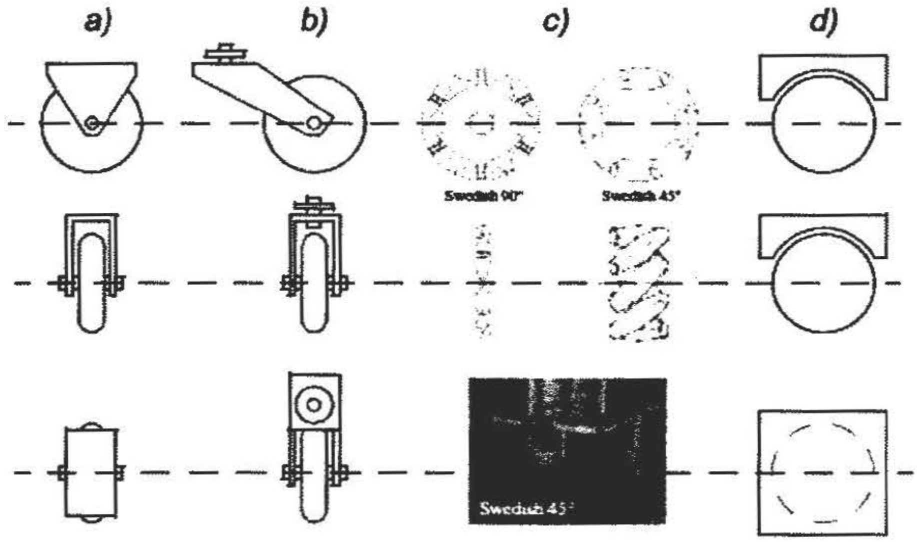

Figure 2.1 The four basic wheel classes
Source: Siegwart and Nourbakhsh, 2004.

Commonly, the kinematics of the mobile robot will depends on the wheel type. The wheel type is crucial when connected to the wheel geometry. In the wheel arrangement is important for develop the kinematic model of the robot. The wheel configuration for rolling vehicles will show in Figure 2.2.

# of wheels	Arrangement	Description	Typical examples
2		One steering wheel in the front, one traction wheel in the rear	Bicycle, motorcycle
		Two-wheel differential drive with the center of mass (COM) below the axle	Cye personal robot
3	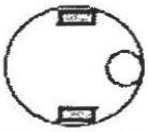	Two-wheel centered differential drive with a third point of contact	Nomad Scout, smartRob EPFL
	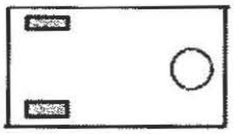	Two independently driven wheels in the rear/front, 1 unpowered omnidirectional wheel in the front/rear	Many indoor robots, including the EPFL robots Pygmalion and Alice
	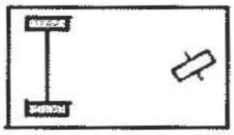	Two connected traction wheels (differential) in rear, 1 steered free wheel in front	Piaggio minitrucks
	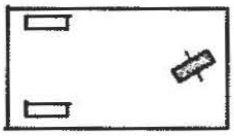	Two free wheels in rear, 1 steered traction wheel in front	Neptune (Carnegie Mellon University), Hero-1
		Three motorized Swedish or spherical wheels arranged in a triangle; omnidirectional movement is possible	Stanford wheel Tribolo EPFL, Palm Pilot Robot Kit (CMU)
	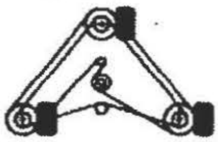	Three synchronously motorized and steered wheels: the orientation is not controllable	"Synchro drive" Denning MRV-2, Georgia Institute of Technology, I-Robot B24, Nomad 200

(a)

# of wheels	Arrangement	Description	Typical examples
4	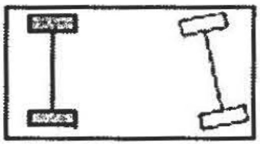	Two motorized wheels in the rear, 2 steered wheels in the front; steering has to be different for the 2 wheels to avoid slipping/skidding.	Car with rear-wheel drive
	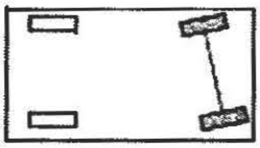	Two motorized and steered wheels in the front, 2 free wheels in the rear; steering has to be different for the 2 wheels to avoid slipping/skidding.	Car with front-wheel drive
	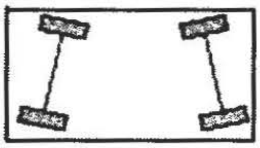	Four steered and motorized wheels	Four-wheel drive, four-wheel steering Hyperion (CMU)
	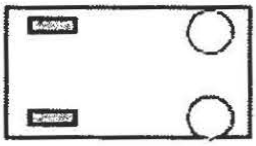	Two traction wheels (differential) in rear/front, 2 omnidirectional wheels in the front/rear	Charlie (DMT-EPFL)
	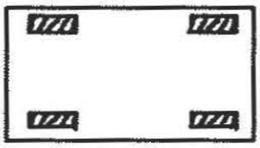	Four omnidirectional wheels	Carnegie Mellon Uranus
	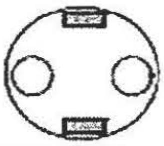	Two-wheel differential drive with 2 additional points of contact	EPFL Khepera, Hyperbot Chip
	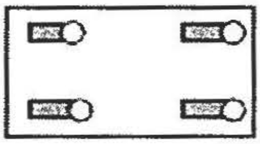	Four motorized and steered castor wheels	Nomad XR4000

(b)

# of wheels	Arrangement	Description	Typical examples
6	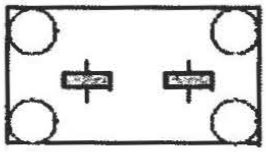	Two motorized and steered wheels aligned in center, 1 omnidirectional wheel at each corner	First
	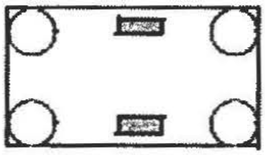	Two traction wheels (differential) in center, 1 omnidirectional wheel at each corner	Terregator (Carnegie Mellon University)
Icons for the each wheel type are as follows:			
	unpowered omnidirectional wheel (spherical, castor, Swedish);		
	motorized Swedish wheel (Stanford wheel);		
	unpowered standard wheel;		
	motorized standard wheel;		
	motorized and steered castor wheel;		
	steered standard wheel;		
	connected wheels.		

(c)

Figure 2.2 (a,b,c)Wheel configurations for rolling vehicles
Source: R.Seigwart & I.Nourbakhsh, 2011

As a research, mobile robot commonly will use three or four wheels for the WMR design. In two wheels have a very simple control but reduce manoeuvrability. While in three wheels have a simple control and steering but limited traction (Ribeiro, Moutinho, Silva, Fraga, & Pereira, 2004).But in four wheels have more complex mechanics and control with high traction (Ribeiro et al., 2004).Thus in two wheels and three wheels are stable but two wheels may not stable balance compare to three wheels. If three or above wheels are used, the mobile robot will encounters an uneven terrain because it allow all wheels to maintain ground contact for a suspension system.

Overall, autonomous mobile robot will use three wheels because due to the simple control and stable balance.

2.2.2 Mathematical Modelling For Wheeled Mobile Robot

The modelling for WMR can divided into two types, kinematics and dynamic equations. Through the mathematical equations, the behaviour and properties for WMR can determine. In kinematic equations, it can describes the localisation or movement of WMR. While in dynamic equations, it can determines the forces and moment of the WMR. So, in a realistic approach, the dynamic model is more appropriate. Extended Kalman Filter had been used to determine the position of a mobile robot and solve the problem through this (Shamrao & Awale, 2016).

2.2.2.1 Kinematic Modelling

Kinematic modelling is commonly used in mathematical technique to describe the movement of WMR. Angular velocity and radius of the wheels have been included in the kinematic modelling. In WMR, the angular velocity can used to derive acceleration and velocity of the movement. The caption of motion control of WMR can determined the difference about the two diving wheel and the angular velocities by using analysis (Mester, 2006). WMR normally works by statically or dynamically when moving it to its destination. Determine the travelling speed and direction to get those destination with the time required for WMR. Basically this is how typical WMR is kinematical controlled (Malu & Majumdar, 2014).

2.2.2.3 Dynamic Modelling

Dynamic modelling of WMR can be classified into several methods in mathematical approach. The first method is the Newton-Euler related the motion of the centre gravity of a WMR with sum of forces and torques acting on the WMR. Base on the relations of angular acceleration and the overall moment of inertia, it is possible to obtain the WMR's dynamic model defined for wheel motor's traction forces, so that can be implemented in the simulation model of mobile robot (CERKALA & JADLOVSKÁ, 2015). Overall, this method is inefficient because only a few of system's forces need to be solved.

The second method is Lagrange dynamic approach, it is very powerful method for formulating the equations of motion in mechanical system. Commonly kinematic and potential energy will use and derive the equation of motion. If those energies are in scalar quantities and it will easy to expressible regarding the system coordinates (Hatab & Dhaouadi, 2013). Therefore, that is not much problem for small multibody systems, while large multibody systems will becomes an efficiency problem.

Another method is Kane's method also can named as Lagrange form of d'Alembert's principle. This principle for developing dynamical equations of motion. In Kane's method offers advantages of both the Lagrange and Newton-Euler methods without disadvantages. The use of generalised forces is eliminates when need to check the interaction and binding forces between the bodies. Therefore, Kane's method will not use energy function, differentiation will not a problem (Meghdari, 2004). The differentiation required to calculate the speed and acceleration can be received by using a vector-based algorithm. Kane's method can provides an elegant way for develop multibody system dynamics equations in automatic numerical calculations (Shamsudin, Mamat, & Nawawi, 2013). Kane's method also used for both holonomic and non-holonomic mobile robot (Kim, Kim, & Kwak, 2005; Song, Fei, & Lu, 2009).

2.3 Microcontroller

Microcontroller is a compact microcomputer designed to govern the operation of embedded systems in motor vehicles, robots, and various other devices. A processor, memory, and peripherals are includes in microcontroller typical.

2.3.1 Arduino

Arduino controller is an easy controller and very familiar to use in the mobile robot. In Arduino controller, there are many types of Arduino board like Arduino UNO (the familiar in all types of project for mobile robot). The advantages for the Arduino UNO can be removed and replaced from the socket in case of breakdown. (Araújo, Couceiro, & Rocha, 2013)The processer for the Arduino UNO is ATmega 328 with 8-bit CPU, 16Mz clock speed, 2KB SRAM, 32KB flash storage. Arduino UNO have 14 digital I/O pins, 6 analog input pins, and removable microcontroller. The Arduino integrated development environmental (IDE) is a cross-platform application written in Java. It can obtained from IDE from the processing programming language and wiring projects(Rajan, Megala, Nandhini, & Priya, 2015).

2.3.2 Raspberry Pi

The Raspberry Pi is a small sized single board computer like credit card size. Currently, in the market, Raspberry PI have five models like Model A, Model A+, Model B, Model B+ and Compute Module. The Raspberry Pi is mainly depended on the same Broadcom BCM2835, SoC (System on Chip – combine with CPU and GPU) but in hardware are difference(SinghPannu, Dawud Ansari, & Gupta, 2015). In Model B+, the operating frequency is 700MHz, memory 512MB SDRAM, 40GPIO pins, 4 USB-2.0 ports and 15pin MIPI camera serial interface with Micro SD card slot(Ujjainiya & Chakravarthi, 2015). The software use in Raspberry Pi is Python. Python is widely use general-purpose, high –level programming language(SinghPannu et al., 2015). For those doing the image processing, the Open CV library need to include it.

2.3.3 NI-myRIO

NI myRIO is a microcontroller which operates based on the dual-core ARM® Cortex™-A9 real-time processing and Xilinx FPGA customizable I/O architecture and provides 256MB of DDR3 memory and 512MB non-volatile memory. The recommended operating external voltage is from 6-16 V for NI myRIO to function. From the physical layout, there are 10 analog inputs, 6 analog outputs, 40 digital I/O lines, Wireless, LEDs, push button, accelerometer on-board. The software using for the NI myRIO is the LabVIEW programming(Mak, 2015). This platform is chosen because it can provide real time data which can be used to compare with the simulated data of the mobile robot.

The compare the difference applications for types of microcontroller will be show at table 2.1

Table 2.1 Difference applications for each microcontroller

	Arduino UNO	**Raspberry Pi**	**NI myRIO**
Analog input	✓	✓	✓
Analog output	×	×	✓
Deterministic (Real Time)	✓	✓	✓
FPGA	×	×	✓

Portable	✓	✓	✓
USB communication	×	✓	✓
WIFI connectivity	×	✓	✓
Linux OS	×	✓	✓
Onboard Processor	×	×	✓
Block Diagram Programming	×	✓	✓

As a result NI myRIO run as Linux OS, this system can having other utilities and allow when configure it with LabVIEW code. NI myRIO can also use to multithreading. In FFGA on the NI myRIO allow run in high-speed data acquisition compare with another microcontroller. Besides, LabVIEW is easily to debug the code than Arduino and Raspberry Pi.

2.4 Platooning Strategy

Platooning is the particular formation of a moving object which has leading and following vehicles. There are no additional data communication between the leading and following vehicles (Klančar, Matko, & Blai, 2011). The following vehicles requires the information regarding the leading vehicles when achieve the platooning. Therefore a combination of both approaches is usually used for this applications (Klančar et al., 2011).

2.5 Sensor Technologies

Autonomous mobile robots mostly using the sensor technologies to senses its surroundings for determine where the position it should be go. The mobile robot must be identify those location within a specified frame of reference, so that the mobile robot will not able to find the way around without the form of sensor. As a result, sensor technologies are most important in mobile robots. In sensor technologies, there are a lot of type sensor using, each sensor have their advantages and disadvantages. So, in this project, choose the best sensor to meet or detecting the object which is meet to the objective.

2.5.1 Range Sensor

Ranger sensor is to detach the changes in its path of sensing. For example ultrasonic sensor is the one of ranger sensor. Ultrasonic sensor can be defined as the electrical- mechanical energy transformation devices. Ultrasonic sensors are used the sound waves rather than light, it will making them ideal for stable detection of uneven surfaces, clear objects, and objects in dirty environments. It is designed for non-contact sensing of strong liquid objects. This information is used to measure between distance and sensor from the object (Goris, 2005; Sabto & Mutib, 2013).

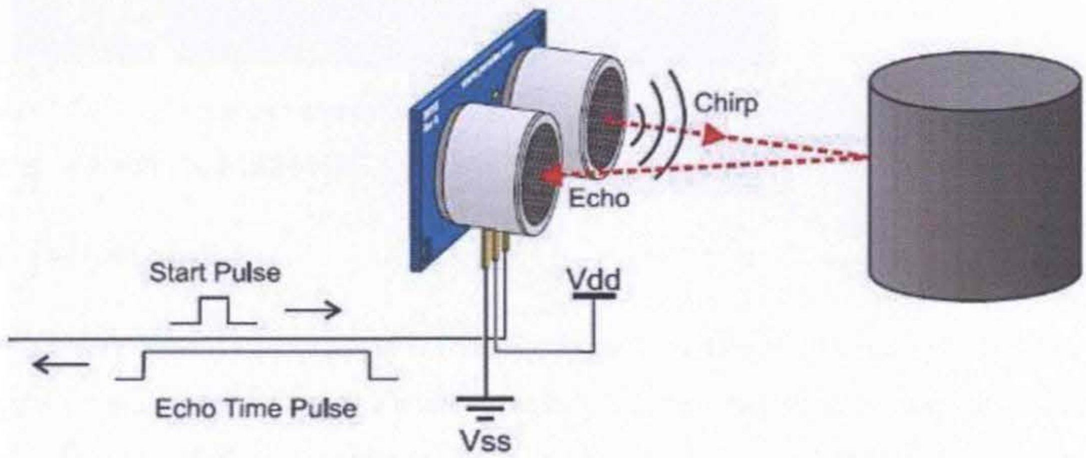

Figure 2.3 Ultrasonic sensor working principle
Source: https://stab-iitb.org/itsprandomap/documentation?id=38

Ultrasonic Sensor sends out a high-frequency sound pulse and then times how long it takes for the echo of the sound to reflect back. This sensor has 2 openings on its front are one opening transmits ultrasonic waves and the other receives them. The speed of sound is approximately 341 meters (1100 feet) per second in air. The ultrasonic sensor uses this information along with the time difference between sending and receiving the sound pulse to determine the distance to an object.

Figure 2.4 Ultrasonic sensor in WMR
Source: N.Sabto, K.Mutib (2013)

2.5.2 Visual Sensor

Visual sensor can to provide in many aspects of data such as colour, motion, voice recognition and objects shape. Visual sensors are commonly used in many fields such as camera. In this world, there are a lot of visual based sensors but the most popular visual sensors is the Kinect. Kinect is widely used because it has certain future that enables it to track the humans. Kinect is developed by Microsoft for the Xbox 360 videogame console and Windows PC for motion sensing. Kinect can be used to recognize human gestures and motion. It has a distinct feature of skeletal tracking which has bone model of the tracked human(Lee, Oh, & Korea, 2014). Figure 2.5 shows the bone model which consists of 20 joints and it corresponded links (Warade, Aghav, Petitpierre, & Udayagiri, 2012).

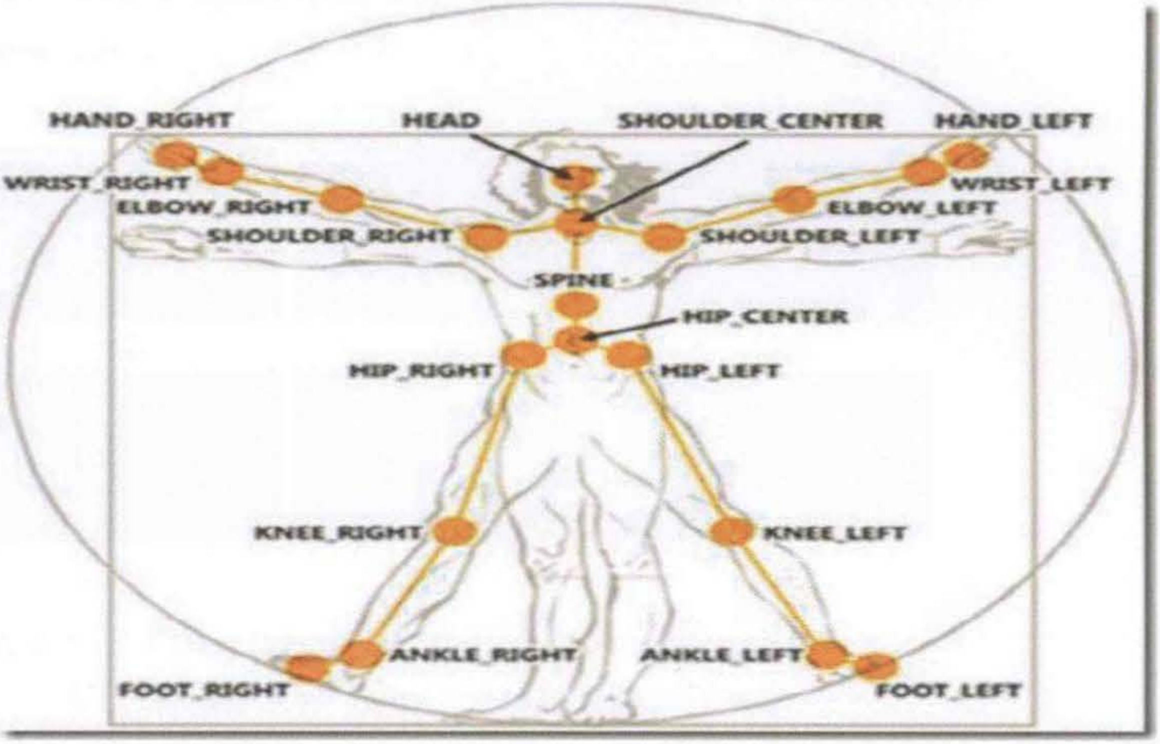

Figure 2.5 Skeleton joint element
Source: S.Lee, S.Oh, S.Korea (2014)

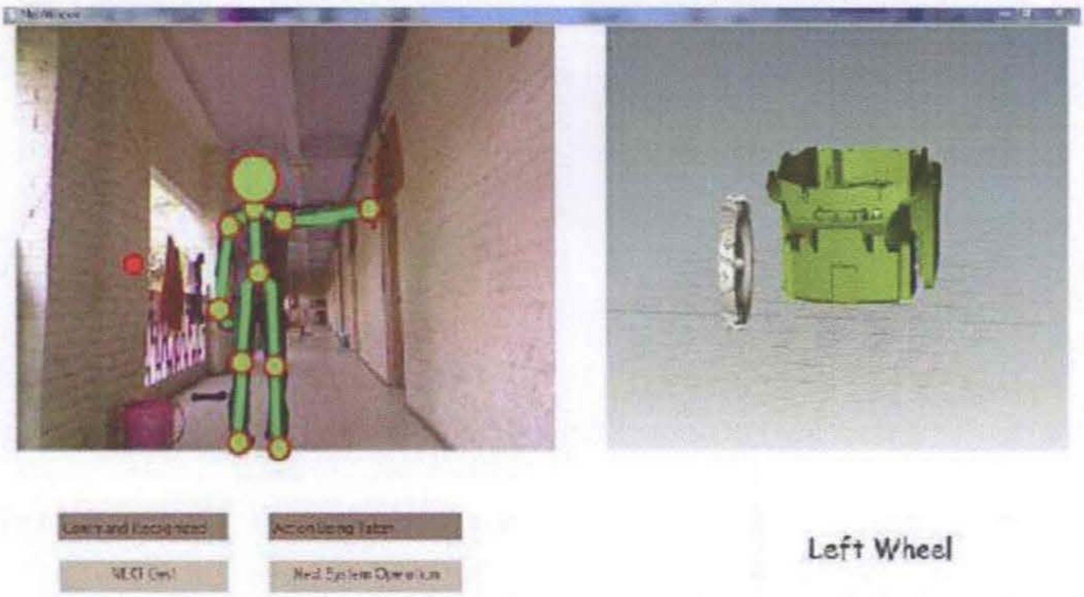

Figure 2.6 Motion control the turning wheel
Source: Warade, Saket (2012)

Another amazing feature of Kinect is that it enables real time tracking information of the joints in 3D. Furthermore, Kinect can simultaneously captures 3D depth images and 2D colour images. Figure 2.7 two scenes typical of the captured data with Kinect (Sharma, 2015).

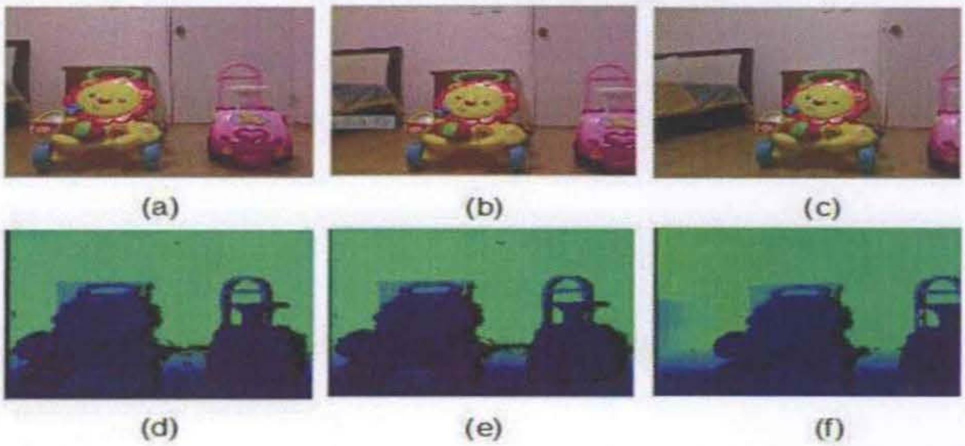

Figure 2.7 Two scenes typical of the captured data with Kinect. (a,b,c) Colour frame and (d,e,f) Depth frame

Source: K. Sharma (2015)

Figure 2.8 Features in Kinect

Source: https://channel9.msdn.com/Series/KinectSDKQuickstarts

Depth Sensing

The depth sensing consists of two parts which is the infrared (IR) laser emitter and the IR camera. A noisy pattern of structured IR light at 830nm is created by the IR laser emitter. In general, the principle of structured light is the basic of the depth sensing. There is a known pseudorandom pattern of dots that are pushed out from the camera. These pushed put dots are recorded by the IR camera and compared with the known pattern. A disturbance in the form of variation in the surface is detected as closer or further away. However, there are several problems which are derived from a central requirement: light matters.

- The wavelength of the emitted IR must be constant.
- Issues with ambient lights.
- Emitter strength limits the sensing distance.

RGB Camera

The RGB camera also can name as colour camera operates at 30Hz and can push images at 640x512 pixels. The resolution of the camera can be adjusted to high by running at 15 frames per second (fps) where in reality it is more to 10fps at 1280x1024 pixels. The former resolution is reduced slightly to match the depth camera. The outputs sent over the USB are in 640x480 pixels and 1280x1024 pixels. Furthermore, the camera possesses features such as automatic white balancing, black reference, flicker avoidance, colour saturation, and defect correction (Tölgyessy & Hubinský, 2010).

After research both of the sensors, an ultrasonic sensors is work on ultrasonic sound waves. Ultrasonic wave will transmitted and hits an object then returns back. The distance needed to calculate form time consumed till the wave returns to the origin. It will give more accurate readings. But there may be some problems if there are sound absorbers with the object or echo is produced due to multiple sound waves returning origin at the same time. While in Kinect sensor is a fast and accurate optical sensor for extracting 3D information from 0.4m to 7.0m compare with other optical depth sensors. Kinect sensor using optical sensor, while in non-optical sensor have to be used to assist "seeing" the crystalline or highly reflective objects. Kinect sensors will read the images from the RGB and depth sensor can fast image processing and achieved with higher computing power. So with this two sensors comparison, the Kinect sensors will more advantages then ultrasonic sensor.

2.6 Summary

Base on the research for those literature review, two wheels will used at the side with the castor wheel at the centre for the base of autonomous mobile robot. The autonomous mobile robot will use three wheels because due to the simple control and stable balance. For the two wheels will be connected with DC motor and controlled using different drive system. The dynamic modelling will be used in simulation with Newton-Euler approach. NI myRIO run as Linux OS, this system can having other utilities and allow when configure it with LabVIEW code. NI myRIO can also use to multithreading. In FFGA on the NI myRIO allow run in high-speed data acquisition. Besides, LabVIEW is easily to debug. Kinect will be choose as a sensor in autonomous mobile robot to detect image and object in 3D.

CHAPTER 3

METHODOLOGY

3.1 Introduction

In this chapter, the topic the will be focused on the mathematical equations and the method that has been used to prove the reliability of this project.

3.2 Methodology Flow Chart

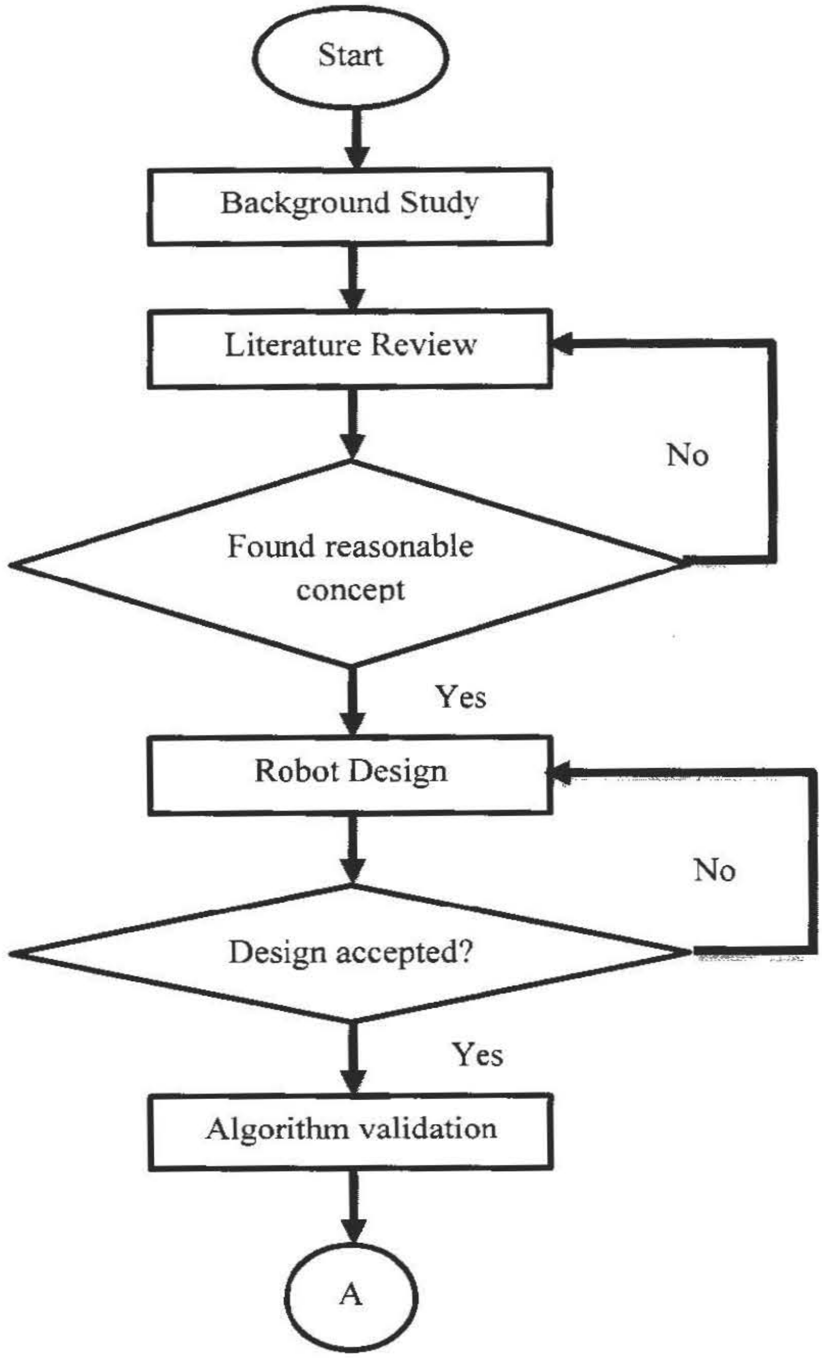

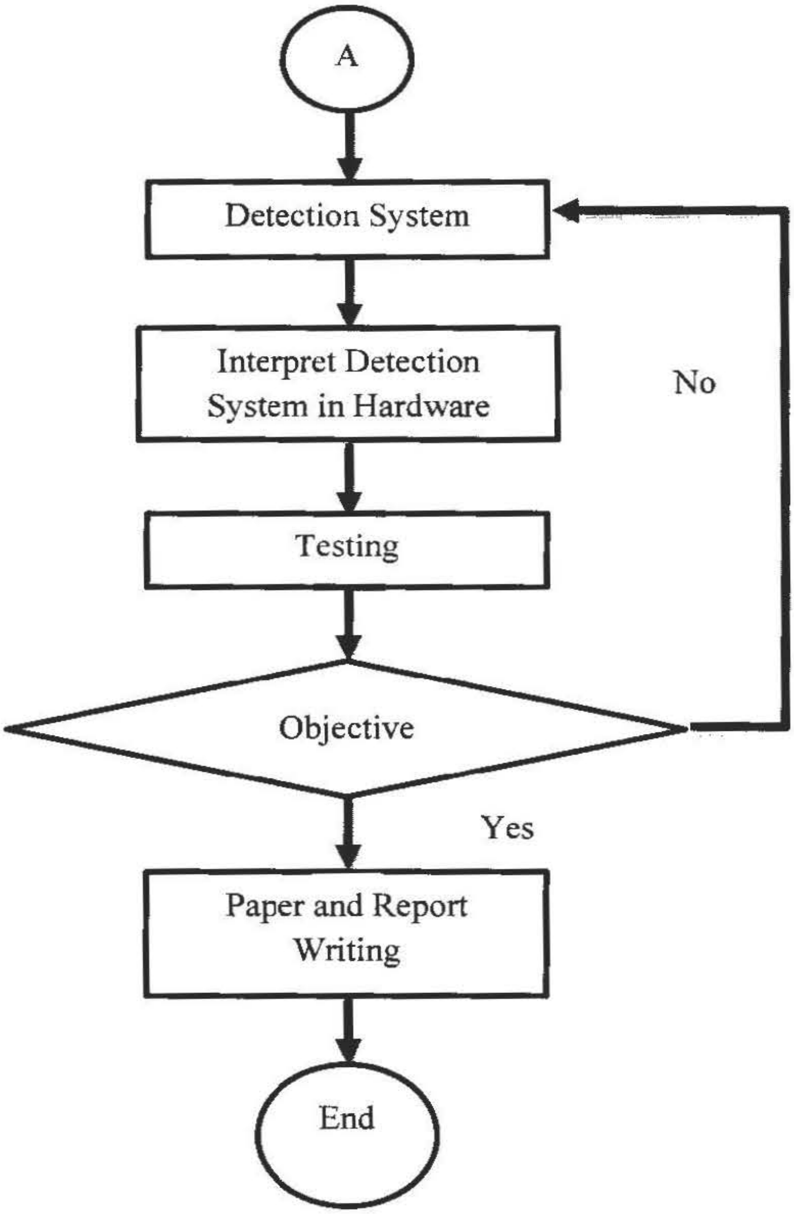

Figure 3.1 Project flow chart

3.3 Hardware Development

3.3.1 Mechanical Development

3.3.1.1 WMR Design Using CATIA

In this project, CATIA is been used to draw/design the basement/frame of mobile robot. The designing crucial to ensure there is no loss of material when developing the actual robot. The mobile robot design is shown in the figure 3.2

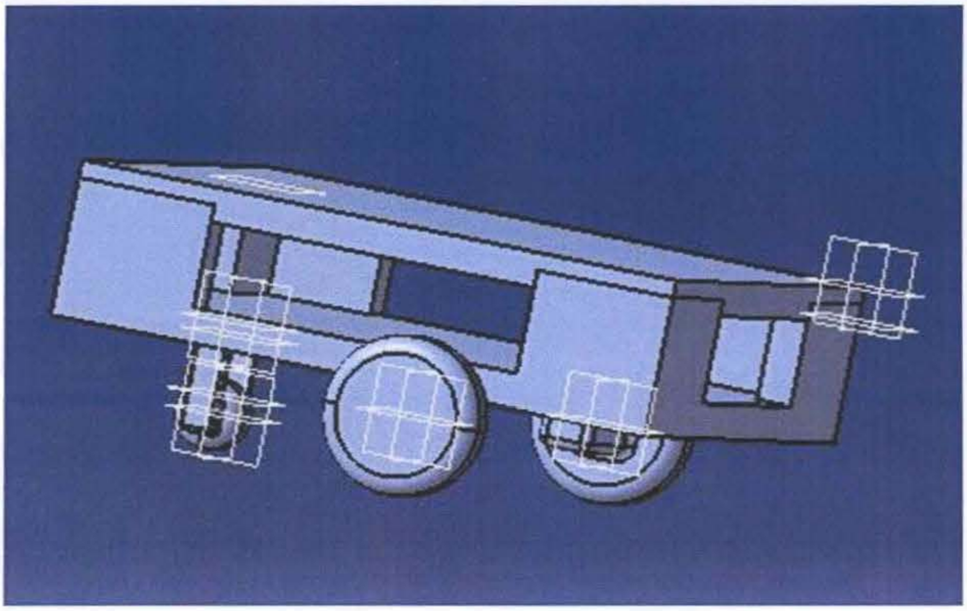

Figure 3.2 Design of mobile robo

The dimension of mobile robot is 300mm x 200mm. A castor wheel will added to the mobile robot as a support.

3.3.2 Equipments

3.3.2.1 NI myRIO

NI myRIO is an embedded hardware device that introduces students to industry proven technology and allows them to design real, complex engineering systems more quickly and affordably than ever before. Besides that, NI myRIO is a microcontroller which operates based on the dual-core ARM® Cortex™-A9 real-time processing and Xilinx FPGA customizable I/O architecture and provides 256MB of DDR3 memory and 512MB nonvolatile memory. The recommended operating external voltage is from 6-16 V for NI myRIO to function. From the physical layout, there are 10 analogue inputs, 6 analogue outputs, 40 digital I/O lines, Wireless, LEDs, push button, accelerometer on board.

This platform is chosen because it can provide real-time data which can be used to compare with the simulated data of the mobile robot.

Figure 3.3 NI myRIO platform

Source: http://sine.ni.com/nips/cds/view/p/lang/en/nid/211694

3.3.2.2 Xbox 360 Microsoft Kinect Sensor Model 1414

Kinect Sensor is an integrated sensor array which is designed by Microsoft as a user interact gaming consoler. It contains of an infrared sensor and high resolution camera which is capable for the input device of the robot's vision system. The reason for choosing the Figure 3.4 shown Xbox 360 Microsoft Kinect sensor.

Figure 3.4 Xbox 360 Microsoft Kinect sensor

Source: https://channel9.msdn.com/Series/KinectSDKQuickstarts

The library for Kinect senor need to install inside the LabVIEW. The model 1414 Xbox 360 Microsoft Kinect sensor only can function through this library after do some research.

3.3.2.3 DC Motor and Wheel

DC motor

DC motor that will selected for WMR is DC geared motor with Encoder SPG30E-30K with a ratio of 30:1 and 103rpm. The motor specification are presented as rated voltage (12V DC), current at free run (no load) with 12V: 70mA, current at loaded (rated), 12V: 410mA and rated Torque: ~1.3 kg.cm (127.4mN.m).

Figure 3.5 DC geared motor with Encoder SPG30E-30K
Source: http://www.cytron.com.my

Wheel

Plastic wheel for SPG30 will used in WMR. This wheel no additional coupling is needed, the centre of rim fit perfectly with D shape 6mm round shaft.

Figure 3.6 Plastic wheel for SPG30
Source: http://www.cytron.com.my

3.3.2.4 DC Motor Drive

SmartDriveDuo10 DC motor driver will be chosen because of the dual channel DC motor driver. SmartDriveDuo10 has the specification of MDD10A which can drive two brush motor at 10A each. The figure 3.7 will show the SmartDriveDuo10 DC motor driver.

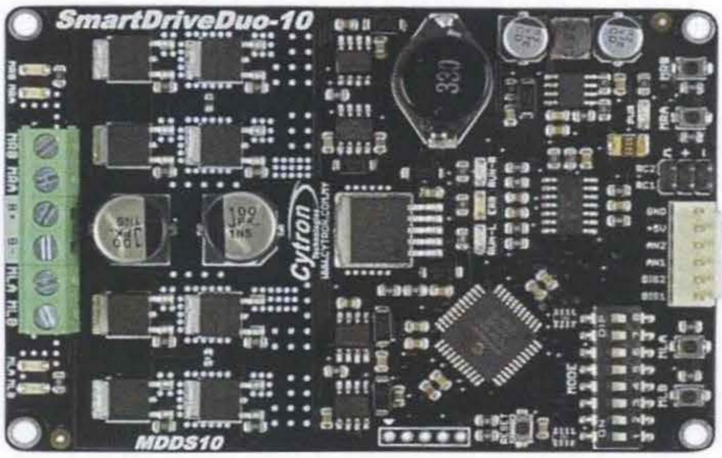

Figure 3.7 SmartDriveDuo10 DC motor driver
Source: http://www.cytron.com.my

3.3.2.5 Power Supply

The power is supplied for this WMR using Lithium Polymer (LiPo) rechargeable battery. LiPo Rechargeable Battery 11.1V 2200mAH will used to this project because small –size and lightweight.

Figure 3.8 LiPo Rechargeable Battery 11.1V 2200mAH
Source: http://www.cytron.com.my

3.3.3 Overall Hardware Structure

The mechanical and equipment with all electrical part of the mobile robot have been assembled and the final output as shown in figure 3.9 (a and b).

(a) (b)

Figure 3.9 (a) Front view mobile robot, (b) Side view mobile robot

3.4 PID Controller

A Proportional-Integral-Derivation controller (PID controller) is a control loop feedback mechanism widely used to control algorithm in industries. PID controller constantly connected for calculates an error value as difference between measured process variable and a desired set point. Besides, PID controller allows users to oprate in a simple and straightforward manner.

In PID controller have three basic algorithm output (proportional, integral and derivative responses) and summing those three components to calculate output. The process diagram for close loop system will shown in figure 3.10.

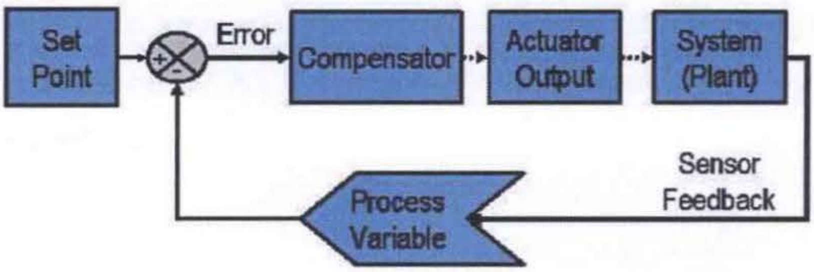

Figure 3.10 Process diagram for close loop system
Source: http://www.ni.com/white-paper/37

3.4.1 PID Theory

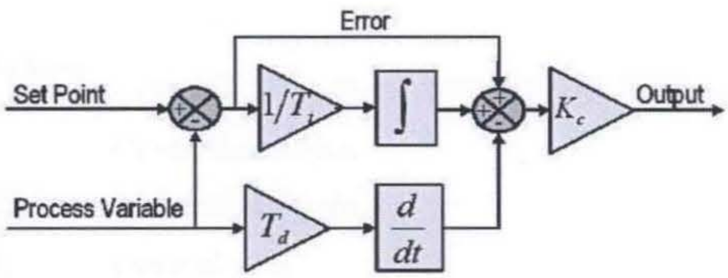

Figure 3.11 Block diagram for a basic PID control alogrithum
Source: http://www.ni.com/white-paper/37

Proportional Term

The proportional term can produces an output value that proportinal to the current error value. The proportional gain constant, K_p as the proportional response can be adjusted by multiplying the error with constant K_p.

$$P_{out} = K_p e(t) \tag{3.1}$$

Integral Term

The integral term is proportional to both the magnitude of error and duration of the error. The accumulated error is then multiplied by the integral gain, K_i and added to the controller output.

$$I_{out} = K_i \int_0^t e(\tau)d\tau \tag{3.2}$$

Derivation Term

The derivative of the process error is calculated by determining the slope of the error over time and multiplying this rate of the change by the derivative gain, K_d. Derivative gain, K_d is a magnitude of the contribution of the derivative term to overall control action.

$$D_{out} = K_d \frac{de(t)}{dt} \tag{3.3}$$

The PID controller algorithm can shown as below:

$$u(t) = MV(t) = K_p e(t) + K_i \int_0^t e(\tau)d\tau + K_d \frac{de(t)}{dt} \tag{3.4}$$

Where

(t)	: Controller output
K_p	: Proportional gain,
K_i	: Integral gain,
K_d	: Derivative gain,
e	: Error
t	: Time or instantaneous time (the present)
τ	: Variable of integration; takes on values from time 0 to t.

3.5 Model Development

There are two types of modelling involved in autonomous mobile robot. The first is the kinematic model of the mobile robot which is influences the differential drive system of the robot. After the kinematic model, the dynamic modelling of the autonomous mobile robot which will includes the electro-mechanical system.

3.5.1 Kinematic Model

Mathematic model

The differential drive model is derived from the forward kinematics equation. It represent elementary model where all physical issues like inertia, friction and mechanical structure inaccuracy are neglected.

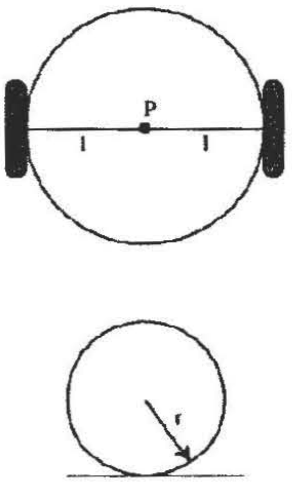

Figure 3.12 The forward kinematic model
Source: Jeffrey Tan Too Chuan and Farrukh Hafiz Nagi, 2005.

Robot motion is defined by the modelling of robot references frame with refer to global inertial reference frame. The point (X_I, Y_I) is an initial point. A point *P* is chosen on the robot chassis as its position reference point. The point (X_R, Y_R) is used to define the axes which are relative to *P*. The point (X_R, Y_R) is also the robot's local reference frame. The position of point *P* in the global reference frame is specified with coordinates *x* and *y*, θ gives the angular difference between the local and the global reference frame.

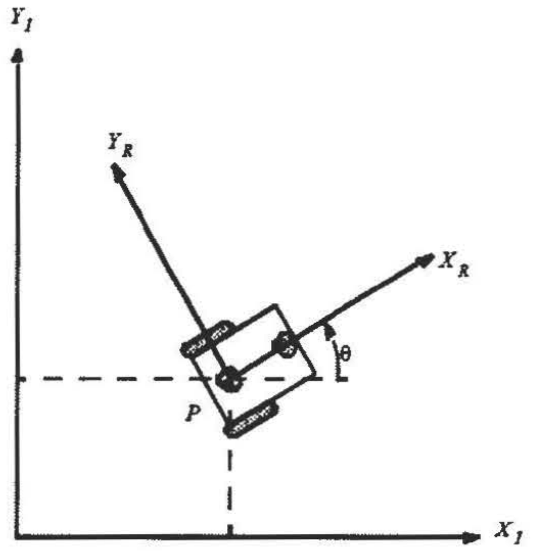

Figure 3.13 Reference frames for robot position
Source: Jeffrey Tan Too Chuan and Farrukh Hafiz Nagi, 2005.

Define the robot motion as below:

$$\dot{\xi}_I = \begin{bmatrix} \dot{x} \\ \dot{y} \\ \dot{\theta} \end{bmatrix} = g(l, r, \theta, \omega_1, \omega_2) \tag{3.5}$$

$$R(\theta) = \begin{pmatrix} \cos(\theta) & \sin(\theta) & 0 \\ -\sin(\theta) & \cos(\theta) & 0 \\ 0 & 0 & 1 \end{pmatrix} \tag{3.6}$$

Thus, describing the motion of the robot between the frames

$$\dot{\xi}_R = R(\theta)\dot{\xi}_I \tag{3.7}$$

$$\therefore \dot{\xi}_I = R(\theta)^{-1}\dot{\xi}_R \tag{3.8}$$

Considering a simple 90° point turn where $\theta = \pi/2$ and substitute into equation (3.6):

$$R(\frac{\pi}{2}) = \begin{bmatrix} 0 & 1 & 0 \\ -1 & 0 & 0 \\ 0 & 0 & 1 \end{bmatrix}$$

$$\therefore \dot{\xi}_R = R\left(\frac{\pi}{2}\right)\dot{\xi}_I = \begin{bmatrix} 0 & 1 & 0 \\ -1 & 0 & 0 \\ 0 & 0 & 1 \end{bmatrix} \begin{bmatrix} \dot{x} \\ \dot{y} \\ \dot{\theta} \end{bmatrix} = \begin{bmatrix} \dot{y} \\ -\dot{x} \\ \dot{\theta} \end{bmatrix} \tag{3.9}$$

Inverting the standard orthogonal rotational transformation for equation (3.6):

$$R(\theta)^{-1} = \begin{bmatrix} \cos(\theta) & -\sin(\theta) & 0 \\ \sin(\theta) & \cos(\theta) & 0 \\ 0 & 0 & 1 \end{bmatrix} \tag{3.10}$$

The model at figure 3.12, the speed of each wheel is $r\omega$ and hence the translational speed is given by the average velocity:

$$\dot{x}_R = r\left(\frac{\omega_1 + \omega_2}{2}\right) \tag{3.11}$$

Instantaneous rotation P for one wheel:

$$\omega_1 = r\frac{\omega_1}{2l} \tag{3.12}$$

The complete rotation:

$$\dot{\theta} = \frac{r}{2l}(\omega_1 - \omega_2) \tag{3.13}$$

Substituting equation (3.9), (3.10), (3.11) and (3.13) into (3.8) to obtain the differential drive model:

$$\dot{\xi}_I = \begin{bmatrix} \cos(\theta) & -\sin(\theta) & 0 \\ \sin(\theta) & \cos(\theta) & 0 \\ 0 & 0 & 1 \end{bmatrix} \frac{r}{2} \begin{bmatrix} \omega_1 + \omega_2 \\ 0 \\ \dfrac{\omega_1 - \omega_2}{l} \end{bmatrix} = \begin{bmatrix} \dot{x} \\ \dot{y} \\ \dot{\theta} \end{bmatrix} \tag{3.14}$$

3.5.2 Dynamic Model

The dynamic model developed was based on Newton-Euler approach. For this model, the chassis robot and DC motors have consists of dynamic behaviour. The model derived is in view of centre of mass dynamics. Besides that, this model broaden standard model dependency of motor supply voltage and wheel speed while including the dynamic part describing. Moreover, chassis and motor were included some parameters such as dynamics and construction with other parameters.

The model was an adaptation from F. Dušek (2011) and the parameters were modified to the model WMR that is developed. The derivation of motion equation is the work for started by taking force balance.

Assuming F (actual force acting) and then the axis of rotation from a mass point with mass m and distance r while add general curvilinear motion where all forces acting vector sum up to a selected point is zero.

$$\vec{F} + \underbrace{\left(m\frac{d\vec{v}}{dt} \right)}_{\substack{Inertial \\ force}} + \underbrace{\left(m\frac{d\vec{\omega}}{dt} \times r \right)}_{\substack{Euler's \\ force}} + \underbrace{\left(2m\vec{\omega} \times \frac{d\vec{r}}{dt} \right)}_{\substack{Coriolis \\ force}} + \underbrace{\left[m\vec{\omega} \times \left(\vec{\omega} \times \vec{r} \right) \right]}_{\substack{Centrifugal \\ force}} = 0 \tag{3.15}$$

Actual conditions is general equation requires specification of individual forces. Curvilinear motion when the forces will be considered to originate from motion of real body when losses in addition.

There are two mathematical model using for dynamic model. Some equations are describe the DC motor rotation speed and the chassis dynamics.

3.5.2.1 Modelling for DC motor

In the autonomous mobile robot have been equipped with two DC motors. The DC motors will connected to the wheels when the constant gear ratio of gear box. The equivalent circuit of a DC motor in series connection is show a figure 3.14.

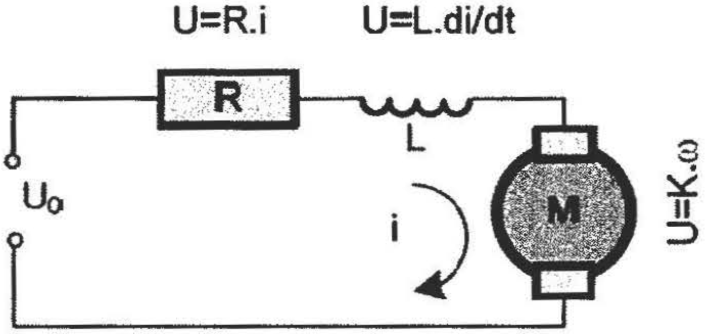

Figure 3.14 Equivalent circuit of motor
Source: F. Dušek (2011)

The above equivalent circuit of DC motor consists of magnetic field of the motor *M*, resistivity *R*, and inductance *L*. The rotor will produces electrical voltage can reverse polarity which develops electromotive voltage *Um*, when proportional to rotor angular velocity *ω*. The losses in magnetic field is not considered however the electric losses will proportional to rotor speed when the winding and mechanical losses. It will be taken into consideration.

Kirchhoff's voltage law will apply for the circuit of the motor drive system is designed and evaluated.

$$U_R + U_L = U_0 - U_M, \quad Ri + L\frac{di}{dt} = U_0 - K\omega \tag{3.16}$$

Where

R	= [Ω] resistance of the motor winding
L	= [H] inductance of the motor
K	= [kg.m2. s-2. A-1] electromotive constant
U0	= [V] voltage of the source
Ω	= [rad. s-1] angular velocity of the rotor

i = [A] current flow in the winding

Next equation as balance of moments (electric energy) with moment of inertia M_S, mechanical losses M_0, motor's load moment M_x and moment due to magnetic field M_M.

$$M_s + M_0 + M_x = M_M$$
$$J\frac{d\omega}{dt} + k_r\omega + M_x = Ki \qquad (3.17)$$

Where

J = [kg.m2] moment of inertia

k_r = [kg.m2. s-1] resistance coefficient of rotation

M_x = [kg.m2. s-2] moment of the load

3.5.2.2 Chassis Dynamics

The chassis dynamics is defined the translation speed vB acting in selected point on the robot body and the angular velocity ωB. In this derivation a point B is taken which is normal projection for the centre of gravity to joint between two wheels as shown in Figure 3.14.

As the starting equation the forces balances is considered. In the derivation, the two forces F_L and F_P acting on chassis at the left (L) and right (P) wheel is ground contact to the points is replaced at force F_B with moment of torque M_B acting to point B. Besides that, the robot body's character is defined with, total mass,m, semi-diameter of the wheels, r, moment of inertia J_T and other parameters with proportional to the centre of gravity such as l_T, l_L, l_p.

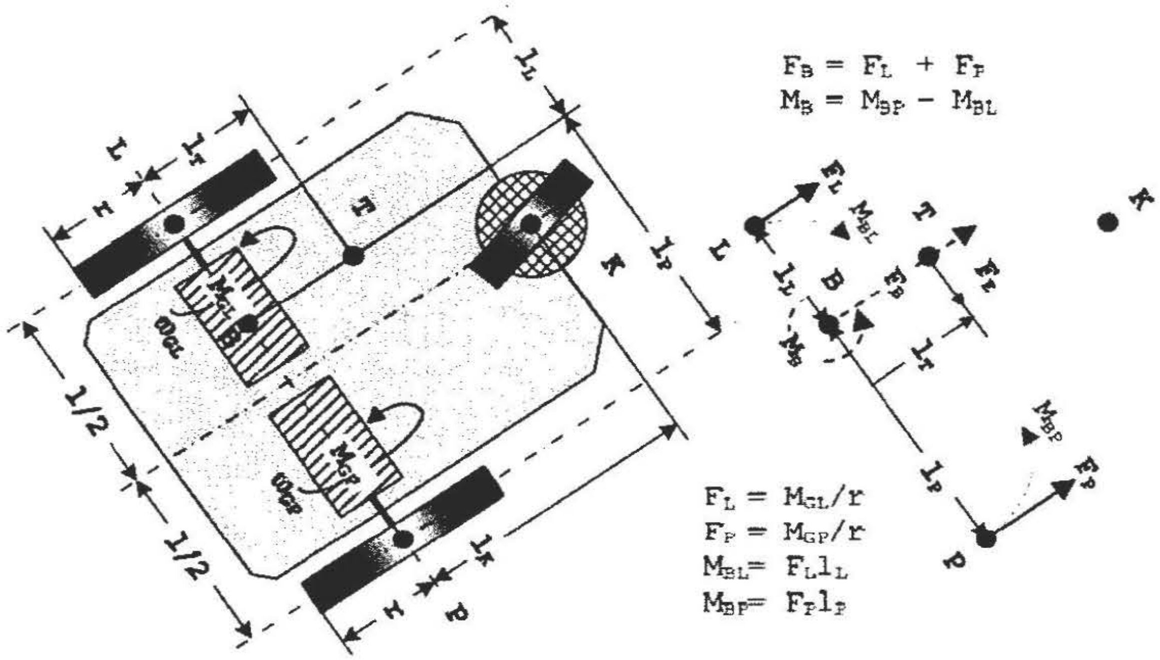

Figure 3.15 Scheme and forces for chassis

Source: F. Dušek (2011)

Where the figure 3.15 showed forces equation;

$$F_L = \frac{M_{GL}}{r}; \quad F_P = \frac{M_{GP}}{r}$$
$$M_{BL} = F_L l_L; \quad M_{BP} = F_P l_P \tag{3.18}$$

$$F_B = F_L + F_P$$
$$M_B = M_{BP} - M_{BL} \tag{3.19}$$

Base on the equation (3.15), the axis of rotation will respect to the position of the centre of gravity is constant, so that Coriolis force no need to consider. Besides that, centrifugal force is ignored because the robot is presumed to be a solid mass. The inertial force through linear motion is adequate since the vector of force initiating the movement acts in point B and travels through centre of gravity. Thus the balance of forces influencing linear motion shown at below equation (3.20).

$$F_L + F_P + F_0 + F_S = 0$$
$$\frac{M_{GL}}{r} + \frac{M_{GP}}{r} - k_v v_B - m\frac{dv_B}{dt} = 0 \tag{3.20}$$

Where

m = [kg] mass of the robot

k_V = [kg. s-1] linear motion's resistance coefficient

M_{GL} = [kg.m2. s-2] left drive's moment

M_{GP} = [kg.m2. s-2] right drive's moment

v_B = [m.s-1] speed of linear motion

r = [m] wheel's semi-diameter.

Balance of moments is not easily achieved because rotation of the axis will not lie in the centre of gravity. Therefore, it necessary to consider chassis momentum M_T and also moment $M_E = l_T F_E$ which is caused by Euler's force F_E. At the same time the moment M_0 is developed with the resistance against rotation and proportional to angular velocity ω_B.

$$\begin{aligned} &M_{BL} + M_{BP} + M_0 + M_T + M_E = 0 \\ &-\frac{M_{GL}}{r} l_L + \frac{M_{GP}}{r} l_P - k_\omega \omega_B - J_T \frac{d\omega_B}{dt} - l_T m \frac{d\omega_B}{dt} l_T = 0 \end{aligned} \tag{3.21}$$

Where

l_P = [m] distance between point B and right wheel,

l_L = [m] distance between point B and left wheel,

l_T = [m] distance between centre of gravity and point B,

k_ω = [kg.m2. s-1] rotary motion's resistance coefficients

J_T = [kg.m2] moment of inertia with respect to rotation axis in centre of gravity

ω_B = [s-1] angular speed in point B.

Base on equation (3.22), rotation axis in point B will respect moment of inertia J_B which is parallel axis theorem or Huygens-Steiner theorem (Horák et al. 1976).

$$J_B = J_T + m l_T^2 \tag{3.22}$$

Where

J_T = [kg.m2] moment of inertia with respect to centre of gravity and

l_T = [m] distance from centre of gravity to point B.

3.5.2.3 Relationship between Motor Speed and Centre of Gravity for Chassis Movement (Kinematic)

The equation is explained the behaviour for two motor and chassis that connected only through moment of engines. Assumed that both wheels are firmly linked to the rotor over ideal gearbox with gear ratio of p_G where no any flexible and nonlinearities members. Therefore, output angular velocity ω_{GX} of the motor reduces due to the transmission with relation to the input angular speed ωx. The output torque M_{GX} increases at the same proportion with relation to the input torque Mx. The equation can be described as shown in equation (3.23) and (3.24).

$$\omega_{GL} = \frac{\omega_L}{p_G}; \quad \omega_{GP} = \frac{\omega_P}{p_G} \tag{3.23}$$

$$M_{GL} = p_G M_L; \quad M_{GP} = p_G M_P \tag{3.24}$$

If the both wheels having a same value of radius r and speeds v_L, v_P will depend on angular speed from gearbox output ω_{GL}, ω_{GP} based on the relations.

$$v_L = r\omega_{GL} = r\frac{\omega_L}{p_G}; \quad v_P = r\omega_{GP} = r\frac{\omega_P}{p_G} \tag{3.25}$$

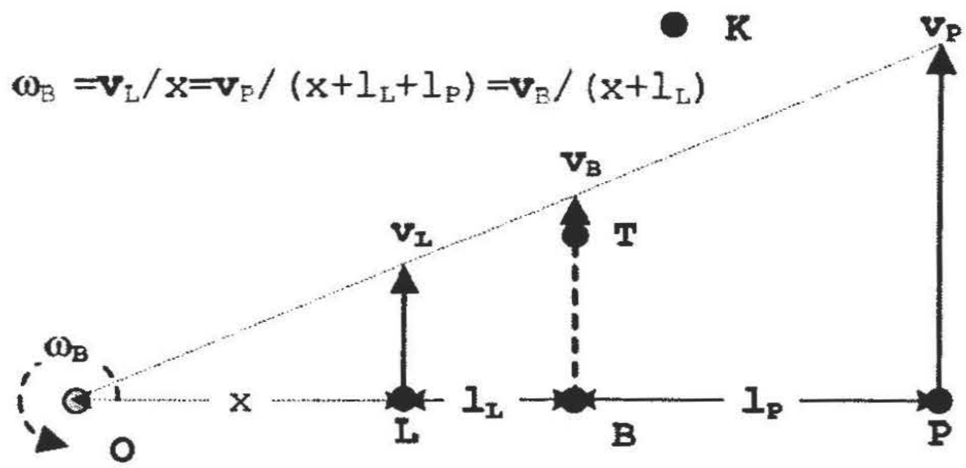

Figure 3.16 Angular speeds and linear recalculations
Source: F. Dušek (2011)

Base on above figure 3.16, the angular velocity of the rotation and the linear speed at point B are derived as equation (3.26) and (3.27)

$$v_B = \frac{V_L l_P + V_P l_L}{l_L + l_P} = \frac{r}{p_G(l_L + l_P)}(l_P \omega_L + l_L \omega_P) \tag{3.26}$$

$$\omega_B = \frac{v_B}{x + l_L} = \frac{v_P - v_L}{l_L + l_P} = \frac{r}{p_G(l_L + l_P)}(-\omega_L + \omega_P) \tag{3.27}$$

3.5.2.4 Trajectory Calculation of the Arbitrary Chassis Points

The linear speed v_B and angular speed ω_B can calculate the current rotation angle α and the current position (x_B,) of point B according to the relations.

$$\frac{d\alpha}{dt} = \omega_B \tag{3.28}$$

$$\frac{dx_B}{dt} = v_B \cos(\alpha) \tag{3.29}$$

$$\frac{dy_B}{dt} = v_B \sin(\alpha) \tag{3.30}$$

Next, for determine all three chassis wheels' points L, P and K for the current position of the contacts in relation to point B as showed at figure 3.17.

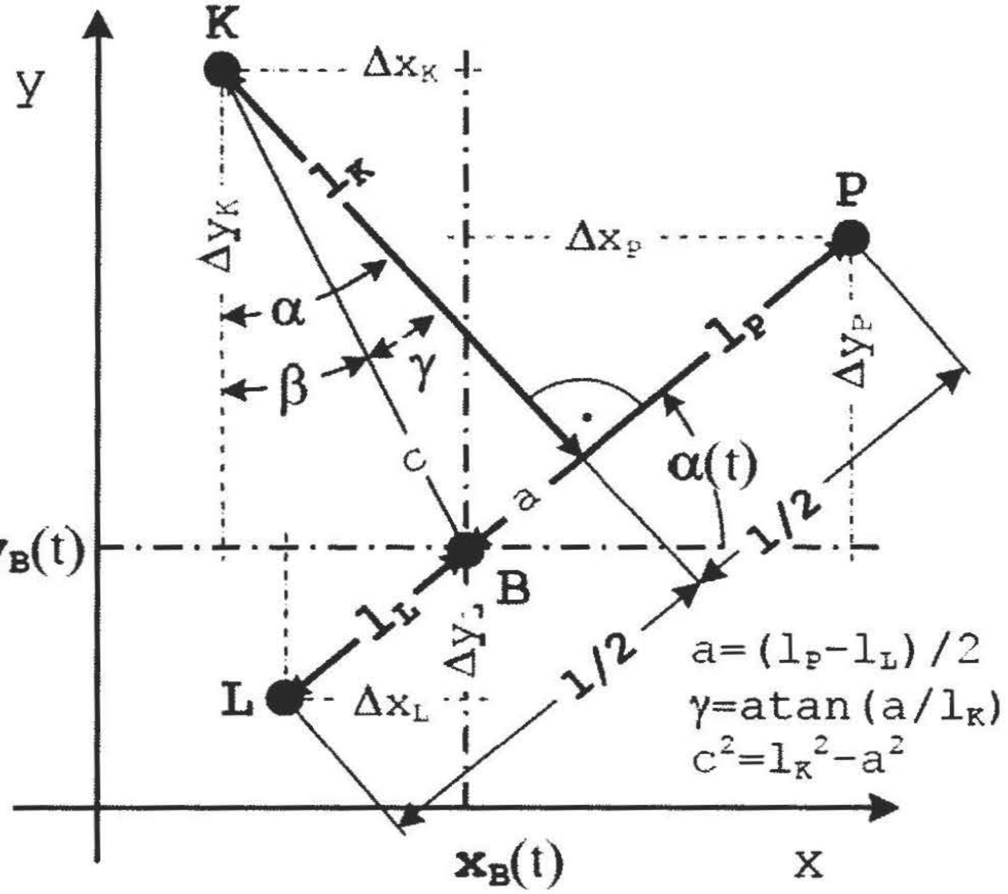

Figure 3.17 Arbitrary chassis point recalculation

Source: F. Dušek (2011)

$$\Delta x_L = -l_L \sin(\alpha); \quad \Delta y_L = -l_L \cos(\alpha) \tag{3.31}$$

$$\Delta x_P = l_P \sin(\alpha); \quad \Delta y_P = l_P \cos(\alpha) \tag{3.32}$$

$$\begin{aligned} &a = \frac{1}{2}(l_P - l_L) \\ &\gamma = \arctan\left(\frac{a}{l_K}\right); \quad c = \sqrt{a^2 + l_K^2} \\ &\Delta x_K = -c\sin(\alpha - \gamma); \quad \Delta y_K = c\cos(\alpha - \gamma) \end{aligned} \tag{3.33}$$

3.5.2.5 Development the Overall Model and Steady-State

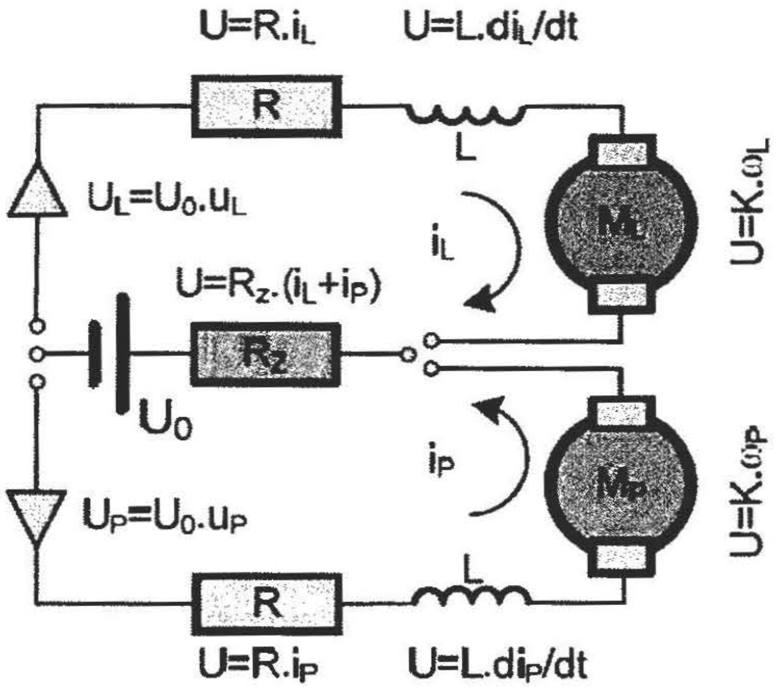

Figure 3.18 Two DC motors wiring

Source: F. Dušek (2011)

Base on the figure 3.18 and using the equations (3.16) and (3.17), come out with 4 differential equations have describing for behaviour of both engines shown as below

$$Ri_L + R_Z(i_L + i_P) + L\frac{di_L}{dt} = u_L U_0 - K\omega_L \tag{3.34}$$

$$Ri_p + R_Z(i_L + i_P) + L\frac{di_P}{dt} = u_P U_0 - K\omega_P \tag{3.35}$$

$$J\frac{d\omega_L}{dt} + k_r\omega_L + M_L = Ki_L \tag{3.36}$$

$$J\frac{d\omega_P}{dt} + k_r\omega_P + M_P = Ki_p \tag{3.37}$$

Base on the equations (3.20) and (3.21) can written with the respect to equations (3.23 to 3.25) and the reduced wheel radius r_G and total moment of inertia J_B as shown in equation (3.38) as below.

$$r_G = \frac{r}{p_G}; \quad J_B = J_T + ml_T^2 \tag{3.38}$$

$$\begin{aligned} &\frac{p_G}{r} M_L + \frac{p_G}{r} M_P - k_v v_B - m\frac{dv_B}{dt} = 0 \\ &M_L + M_p - r_G k_v v_B - r_G m\frac{dv_B}{dt} = 0 \end{aligned} \tag{3.39}$$

$$\begin{aligned} &-l_L \frac{p_G}{r} M_L + l_P \frac{p_G}{r} M_P - k_\omega \omega_B - (J_T + ml_T^2)\frac{d\omega_B}{dt} = 0 \\ &-l_L M_L + l_P M_P - k_\omega \omega_B - r_G J_B \frac{d\omega_B}{dt} = 0 \end{aligned} \tag{3.40}$$

The substitution for the equations (3.26) and (3.27) is rewritten using equation (3.38).

$$v_B = \frac{r_G}{l_L + l_P}(l_P \omega_L + l_L \omega_P) \tag{3.41}$$

$$\omega_B = \frac{r_G}{l_L + l_P}(-\omega_L + \omega_P) \tag{3.42}$$

The six differential equations (3.34,3.35), (3.36,3.37), (3.39,3.40) and two algebraic equations (3.41,3.42) is dynamic behaviour of ideal differentially steered mobile robot with linear losses that contains eight state variables representing a mathematical description which is dependent on speed or revolutions. The input variables are the control signals u_L and u_P which is the supply voltages to the individual motors. Next, Speed of the robot movement v_B and speed of rotation of wheels ω_B as the output variables.

The equations (3.28-3.30) are used to derive the steady-state since the equations as linear with respect to state variables. Therefore, the steady-state is represented in matrix form as shown in equation (3.43).

$$
\begin{bmatrix}
R+R_z & R_z & K & 0 & 0 & 0 & 0 & 0 \\
R_z & R+R_z & 0 & K & 0 & 0 & 0 & 0 \\
K & 0 & -k_r & 0 & -1 & 0 & 0 & 0 \\
0 & K & 0 & -k_r & 0 & -1 & 0 & 0 \\
0 & 0 & 0 & 0 & 1 & 1 & -r_G k_v & 0 \\
0 & 0 & 0 & 0 & -l_L & l_P & 0 & -r_G k_\omega \\
0 & 0 & l_P & l_L & 0 & 0 & -\dfrac{l_P+l_L}{r_G} & 0 \\
0 & 0 & -1 & 1 & 0 & 0 & 0 & -\dfrac{l_P+l_L}{r_G}
\end{bmatrix}
\begin{bmatrix} i_L \\ i_P \\ \omega_L \\ \omega_P \\ M_L \\ M_P \\ v_B \\ \omega_B \end{bmatrix}
=
\begin{bmatrix} U_L \\ U_P \\ 0 \\ 0 \\ 0 \\ 0 \\ 0 \\ 0 \end{bmatrix}
\tag{3.43}
$$

The model of linear part can be modified into easy form by substituting equations (3.41, 3.42) into (3.39, 3.40) and eliminate moments M_L and M_P by substituting equations (3.36, 3.37) to (3.39, 3.40). Thus the four differential equations (3.36, 3.37) to (3.39, 3.40) is reduced into two (3.49). The parameters shown as below.

$$a_L = k_r + \frac{k_v l_P r_G^2}{l_L + l_P}; \quad a_P = k_r + \frac{k_v l_L r_G^2}{l_L + l_P} \tag{3.44}$$

$$b_L = J + \frac{m l_P r_G^2}{l_L + l_P}; \quad b_P = J + \frac{m l_L r_G^2}{l_L + l_P} \tag{3.45}$$

$$c_L = k_r l_L + \frac{k_\omega r_G^2}{l_L + l_P}; \quad c_P = k_r l_P + \frac{k_\omega r_G^2}{l_L + l_P} \tag{3.46}$$

$$d_L = Jl_L + \frac{J_B r_G^2}{l_L + l_P}; \quad d_P = J_P + \frac{J_B r_G^2}{l_L + l_P} \tag{3.47}$$

The reduce linear part of the model equations shown as below

$$
\begin{aligned}
\frac{di_L}{dt} &= \frac{u_L U_0 - K.\omega_L - (R+R_Z).i_L - R_Z i_P}{L} \\
\frac{di_P}{dt} &= \frac{u_P U_0 - K.\omega_P - (R+R_Z).i_P - R_Z i_L}{L}
\end{aligned}
\tag{3.48}
$$

$$
\begin{aligned}
\frac{d\omega_L}{dt} &= \frac{1}{b_L d_P + b_P d_L}\begin{pmatrix} d_P\left[K(i_L+i_P) - a_L\omega_L - a_P\omega_P\right] \\ -b_P\left[K(-l_L i_L + l_P i_P) + c_L\omega_L - c_P\omega_P\right] \end{pmatrix} \\
\frac{d\omega_P}{dt} &= \frac{1}{b_L d_P + b_P d_L}\begin{pmatrix} d_L\left[K(i_L+i_P) - a_L\omega_L - a_P\omega_P\right] \\ +b_L\left[K(-l_L i_L + l_P i_P) + c_L\omega_L - c_P\omega_P\right] \end{pmatrix}
\end{aligned}
\tag{3.49}
$$

The reduced linear part is presented in standard state-space model in matrix from as shown in equation (3.50).

$$
\begin{aligned}
&\frac{dx}{dt} = Ax + Bu \\
&y = Cx \\
&where \\
&x = \begin{bmatrix} i_L \\ i_P \\ \omega_L \\ \omega_P \end{bmatrix} \quad u = \begin{bmatrix} u_L \\ u_P \end{bmatrix} \quad y = \begin{bmatrix} v_B \\ \omega_B \end{bmatrix}
\end{aligned} \tag{3.50}
$$

Constant of matrices in A, B and C will show as below

$$
A = \begin{bmatrix}
-\frac{R+R_Z}{L} & -\frac{R_Z}{L} & -\frac{K}{L} & 0 \\
-\frac{R_Z}{L} & -\frac{R+R_Z}{L} & 0 & -\frac{K}{L} \\
\frac{K(d_P + b_P l_L)}{b_L d_P + b_P d_L} & \frac{K(d_P - b_P l_P)}{b_L d_P + b_P d_L} & -\frac{d_P a_L + b_P c_L}{b_L d_P + b_P d_L} & -\frac{d_P a_P - b_P c_P}{b_L d_P + b_P d_L} \\
\frac{K(d_L - b_L l_L)}{b_L d_P + b_P d_L} & \frac{K(d_L + b_L l_P)}{b_L d_P + b_P d_L} & -\frac{d_L a_L - b_L c_L}{b_L d_P + b_P d_L} & -\frac{d_L a_P + b_L c_P}{b_L d_P + b_P d_L}
\end{bmatrix}
$$

$$
B = \begin{bmatrix}
\frac{U_0}{L} & 0 \\
0 & \frac{U_0}{L} \\
0 & 0 \\
0 & 0
\end{bmatrix}
$$

$$
C = \begin{bmatrix}
0 & 0 & \frac{l_P r_G}{l_L + l_P} & \frac{l_L r_G}{l_L + l_P} \\
0 & 0 & -\frac{r_G}{l_L + l_P} & \frac{r_G}{l_L + l_P}
\end{bmatrix}
$$

3.6 Kinect

3.6.1 Data Processing For Capture Image

There are three resolutions will support by the depth stream such as 640 x 480 pixels, 320 x 240 pixels, and 80 x 60 pixels. While the camera plane at a particular (x, y) coordinate when the depth data contains the distance information to the nearest object. Besides that, depth sensor's field of view range remains the same as the field of view of color camera. an IR emitter and an IR depth sensor that is a monochrome CMOS (Complementary Metal-Oxide- Semiconductor) sensor to capture the 3D information of an object for the Kinect sensors. Depth data processing are detailed will show as below figure 3.19.

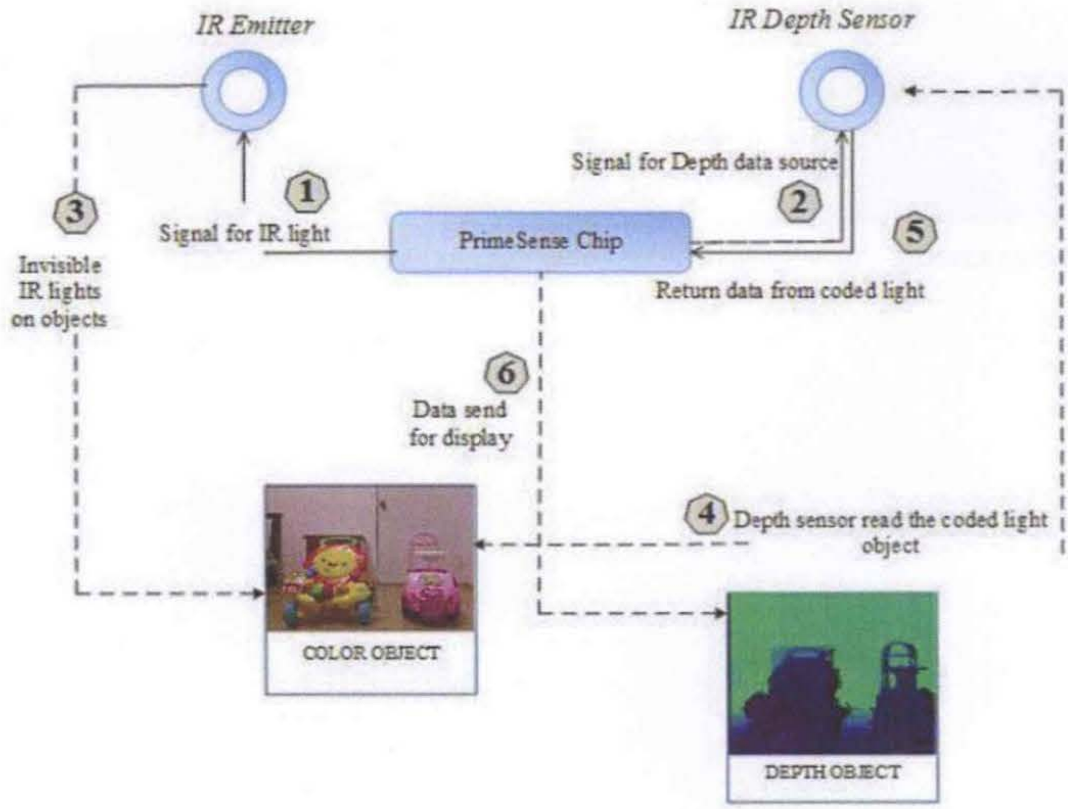

Figure 3.19 Data processing for Kinect
Source: K. Sharma (2015)

3.7 Working Principle of the Mobile Robot

The LabVIEW simulation have been done at laptop and using the Wi-Fi system to transfer the data for myRIO. The myRIO will receives the data and process it. The mobile robot will start moving and the Kinect sensor will start to record video while the ultrasonic will obstacle the object. The video that have record will send feedback to the user interface wall at the LabVIEW simulation. The distance that ultrasonic sensor detect is 20cm. So that the mobile robot will away from the object.

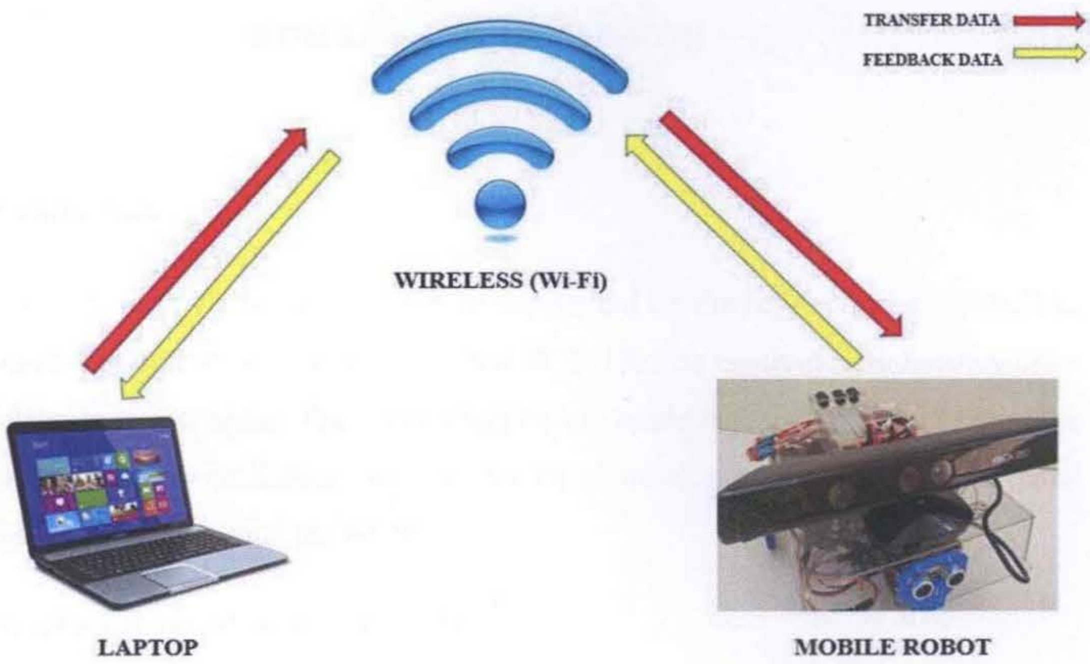

Figure 3.20 Flow of the system

CHAPTER 4

RESULTS AND DISCUSSION

4.1 Introduction

In this chapter, the discussion will be conducted on the results and analysis. The software used for simulation is done in LabVIEW 2013. The result of simulation will be discussed later in this chapter. The block diagram are made in LabVIEW for getting the image and depth data from Kinect then transfer the simulation to myRIO. The simulated system will tested out the data on WMR.

4.2 Simulation and Results for WMR

The simulation at the LabVIEW as shown in Appendix B. The block diagram arranged and the simulation was conducted as shown in Appendix B. While the calculation and the PID control that using WMR as shown in Appendix B. In Appendix B, the quadrature encoder have been used to provide closed loop feedback for position and velocity controlled applications at motor driver control system. While using quadrature encoder for velocity and acceleration control in high speed and precision applications, it can process quadrature encoder signals (velocity, acceleration and instantaneously output controls signals) at hardware timed precision. Simulation for the encoder part shown in figure 4.1.

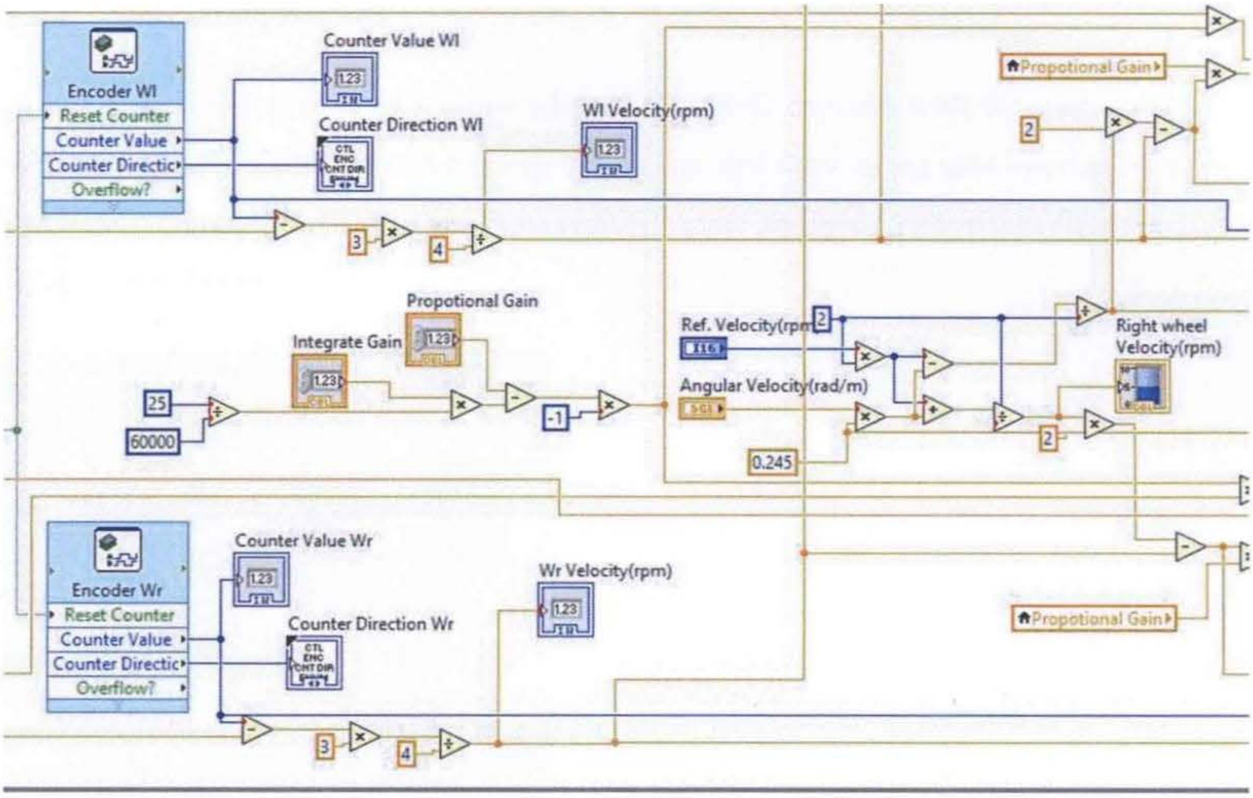

Figure 4.1 Encoder part in simulation

The user interface wall in LabVIEW simulation for PWM signals in rpm and observe the motor response shown in figure 4.2.

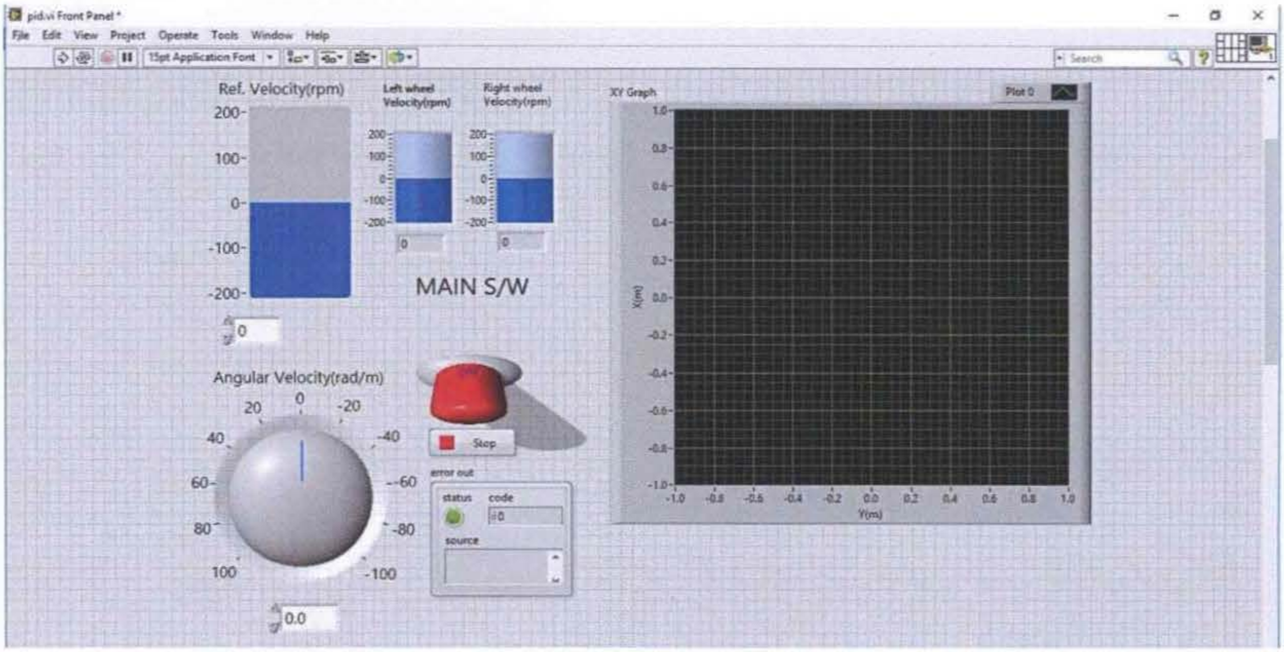

Figure 4.2 The user interface wall in LabVIEW simulation

4.2.1 Simulation Results

The simulation results taken when the myRIO connect with the motor drivers WMR. When the motor drivers turning, the results will show in the user interface wall in LabVIEW simulation. There are three results in this simulation shown in figure 4.3 to figure 4.8 as below.

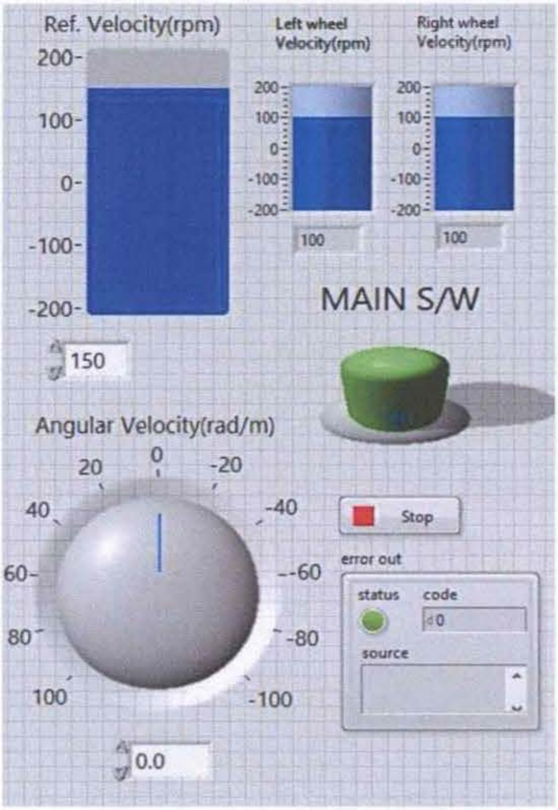

Figure 4.3 The left wheel and right wheel velocity (rpm) and angular velocity

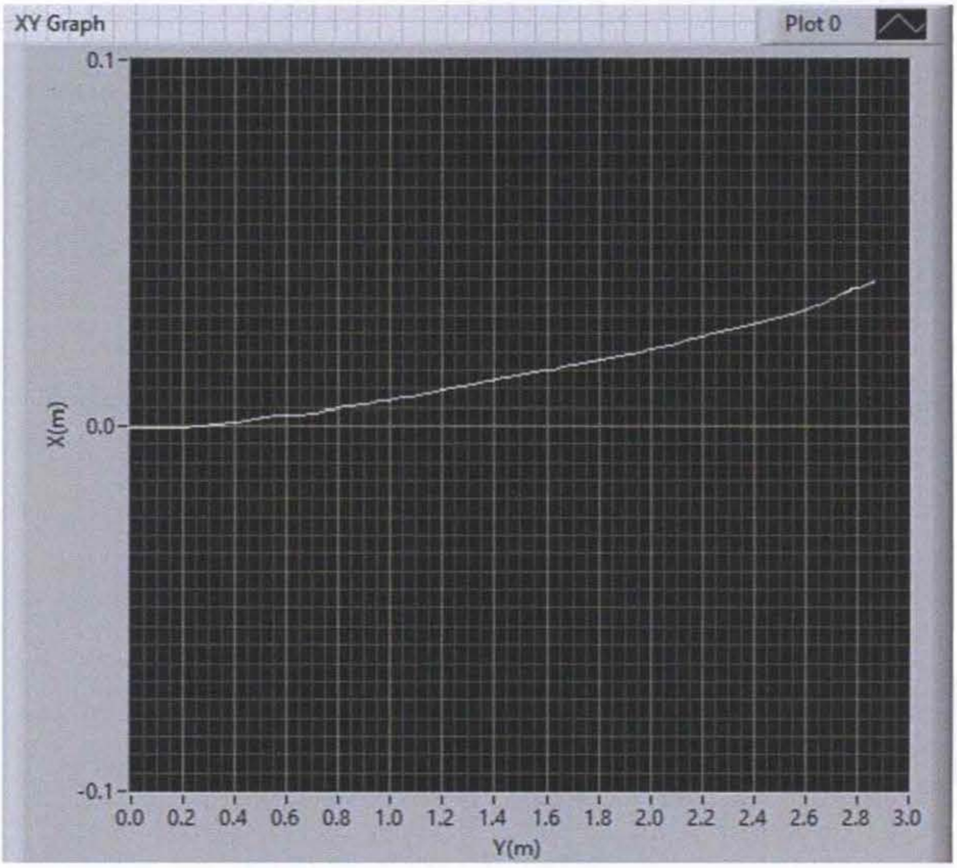

Figure 4.4 WMR motion respect to X and Y coordinate (straight line)

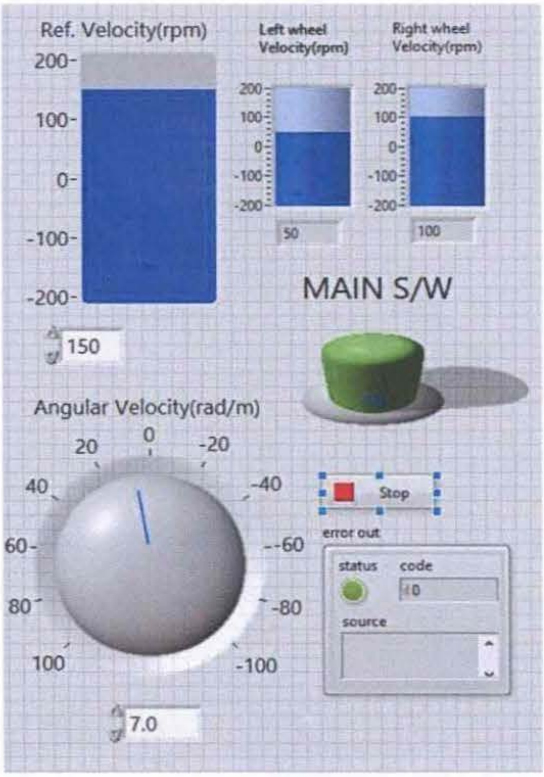

Figure 4.5 The left wheel and right wheel velocity (rpm) and angular vel

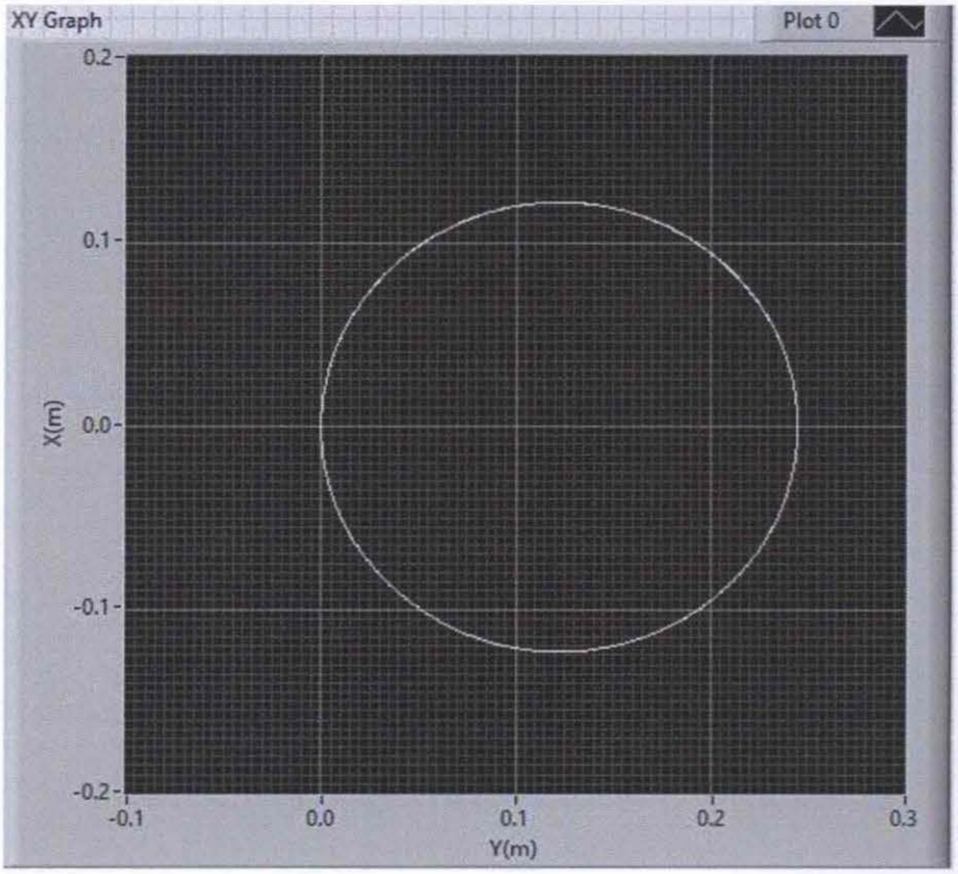

Figure 4.6 WMR motion respect to X and Y coordinate (left direction)

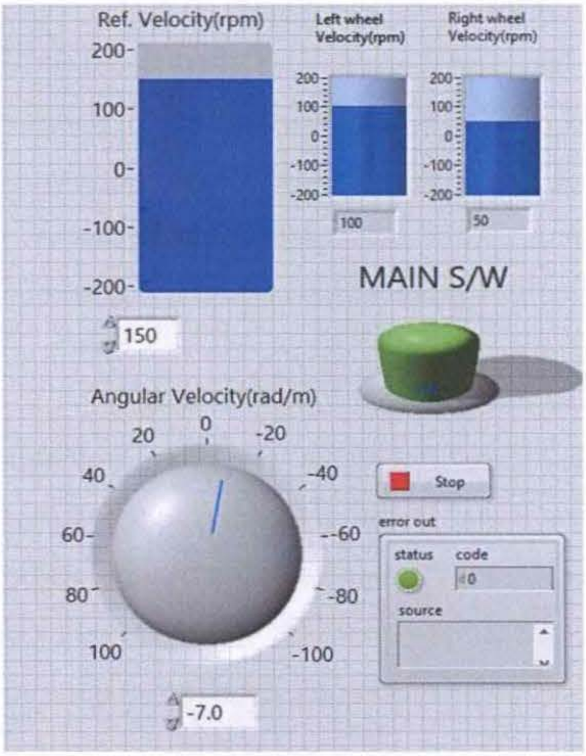

Figure 4.7 The left wheel and right wheel velocity (rpm) and angular velocity

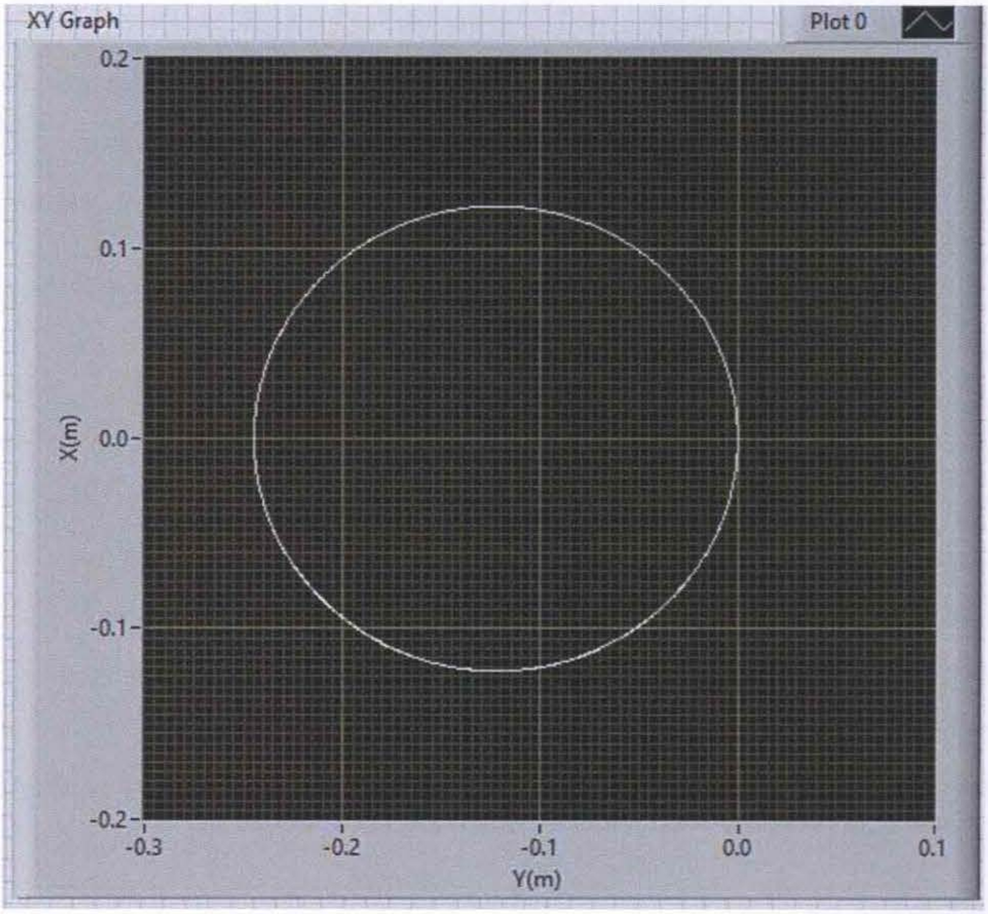

Figure 4.8 WMR motion respect to X and Y coordinate (right direction)

Base on figure 4.3, the first user interface wall shows the left and right wheel in constant velocity (100 rpm). The speed of the wheels remain constant as long as the velocity is same for both wheels. The WMR will move in linearly position. Figure 4.4 shows that WMR motion respect to X and Y coordinate. Normally, X and Y should be constant when take the result. But the graph at X-axis is small increasing due to the initial slip when the motor starts running. Therefore the mobile robot head to left in small angle.

Figure 4.5 show the angular velocity is 7 rad/m that calculate by using the equation in Chapter 3. The left wheel velocity is 50 rpm but right wheel velocity is 100 rpm and cause the right wheel move faster speed than the left wheel. In this situation, create a motion toward to left side. Other than that, the X and Y coordinates shown a circular motion in left direction that shown in figure 4.6. As a result, the mobile robot is moving towards left and become circular pattern.

Figure 4.7 show the angular velocity is -7 rad/m. The left wheel velocity is 100 rpm but right wheel velocity is 50 rpm and cause the left wheel move faster speed than the right wheel. This cause the right wheel will slow and left wheel turn to right side. Furthermore, in figure 4.8 the X and Y coordinates shown a circular motion in right direction. As a result, the mobile robot is moving towards right and become circular pattern.

4.3 Result for Ultrasonic Sensor

Ultrasonic sensor used at the mobile robot with connected to myRIO for obstacle avoidance. LabVIEW simulation for ultrasonic sensor to avoid the object as shown in Appendix C. Thought this simulation, the ultrasonic sensor can avoid the distance between the object and mobile robot. In order to generate the ultrasonic in simulation, the Trig need to set at high state for 10μs and Echo output will be in microseconds sound wave travelled. Therefore, to obtain the time taken between the object and mobile robot, there are some data that taken from simulation and using the mathematic calculation to get time taken that needed. Table 4.1 shows the results in Echo (μs) by ultrasonic sensor.

Table 4.1 Echo(μs) results

No	Time taken (μs)	Distance (cm)
1.	1764	30
2.	1470	25
3.	1176	20
4.	882	15

Mathematic formula to calculate the distance is time taken (μs) multiple by speed of sound (340 m/s or 0.034 cm/ μs) and divided by 2 because sound wave need to travel forward and backward. Figure 4.9 and 4.10 are shows the mobile robot stop at 20 cm from the obstacle (wall) which is equivalent to 1176 μs.

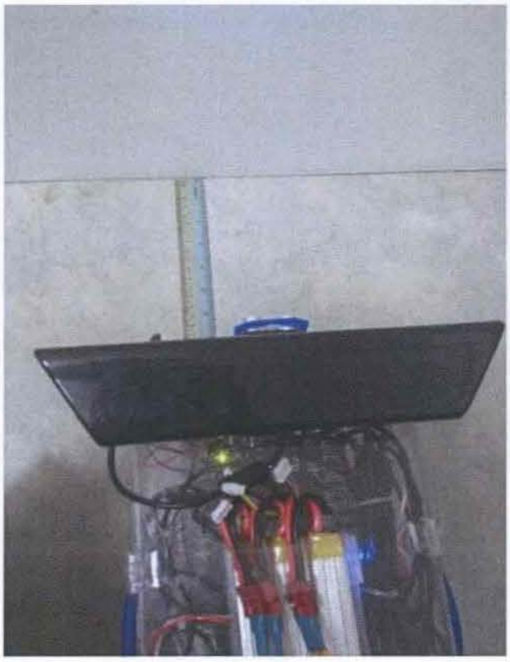

Figure 4.9 Top view for the obstacle result at 20 cm

Figure 4.10 Side view shown the mobile robot stop at 20 cm

4.4 Result for Kinect Sensor

LabVIEW simulation for Kinect sensor to record video and capture image as shown in Appendix D while the hardware part shown in Chapter 3. USB Kinect sensor must connect to myRIO, but before that, library for Kinect sensor must install in myRIO. The library are based on the model 1414 Kinect sensor. Kinect sensor will start to capture video when run through simulation. The user interface for Kinect sensor will shows in figure 4.11. While video and image capture shown in figure 4.12. Table 4.2 shown experimental parameter used.

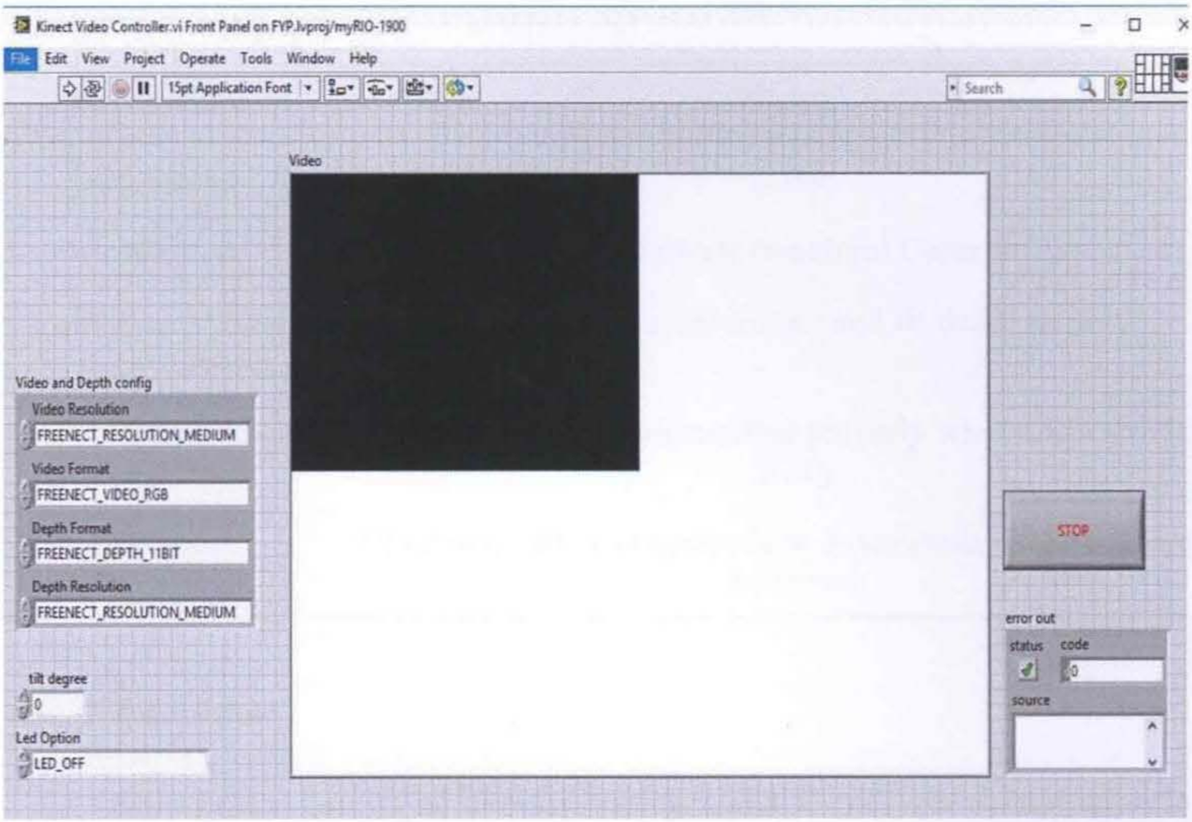

Figure 4.11 User interface wall for Kinect sensor

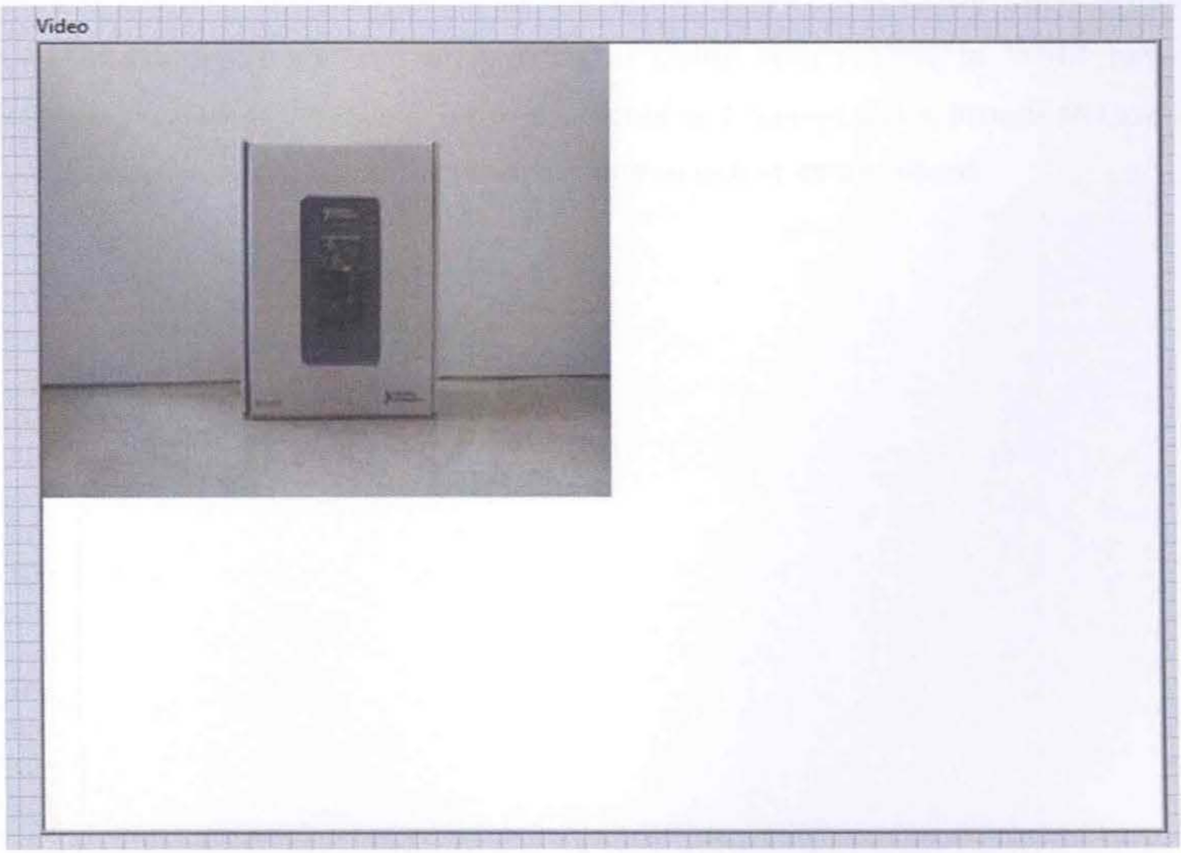

Figure 4.12 Part of video record when mobile robot moving

Table 4.2 Experimental parameter used

Parameters	Value
Data Stream	Color
Resolution	640 x 480 pixels (medium) Color image
Components used in Kinect sensor	Color camera, IR emitter and IR depth sensor
LED	Kinect device drivers installed properly when LED turn into green
Tilt motor	Tilted vertically can upwards or downwards by 27 degrees of the motor

4.5 Discussion

Base on the results of ultrasonic sensor and Kinect sensor that apply on the LabVIEW simulation and real testing. The Kinect sensor will act as the eyes of the WMR and will record all the data. This data can download and showed to the user that WMR is moving from one places to another places. While the ultrasonic sensor will help the WMR to obstacle object and can away from it. Using both sensors in WMR have more advantages such as the mobile robot can record and capture all the images and away from the distance between an object when moving in indoor environment.

CHAPTER 5

CONCLUSION AND RECOMMENDATIONS

5.1 Conclusion

The autonomous mobile robot using myRIO have been discussed in this research. The kinematic and dynamic equations have been discussed and derived based on the previous studies. Both equations were used in WMR mobile robot and apply in the LabVIEW simulation. The results were successfully obtained through the implementation both equations. PID controller have been used in LabVIEW simulation and successfully control the mobile robot to move in constant speed. Besides, the Kinect sensor and ultrasonic sensor in LabVIEW simulation have been successful apply in mobile robot through myRIO hardware. The autonomous mobile robot hardware have successfully install with all components that haven been mentioned before.

Base on the objective in chapter 1, the autonomous mobile robot have been designed to suit in indoor environment. The size of mobile robot is designed to move in indoor environment. Next, Kinect sensor and ultrasonic sensor were successful apply in mobile robot. Kinect sensor can capture image and record video when mobile robot moving. While ultrasonic sensor can detect the obstacle. The most important is the PID controller also successfully implementation in mobile robot control. Finally, the LabVIEW simulation were successfully designed and applied in the myRIO hardware. The mobile robot was able to move when through the Wi-Fi to transfer data from computer to myRIO hardware.

To conclude, autonomous mobile robot have been successfully developed. The experiment results have been successfully recorded. However, simulation results are slightly different compared to the real-time implementation as the simulation lack of additional external factors that change the obtained results. Besides that, when doing

LabVIEW simulation, most challenge was the LabVIEW system because LabVIEW have a lot of block diagram and special icon. The time for research LabVIEW was used a lot and understand it. Moreover, using Wi-Fi to transfer data was no stable compare using USB from computer. The data will delay when using Wi-Fi and the mobile robot will delay. In a whole, the mobile robot was successful capture image, record video and obstacle object.

5.2 Recommendations

The mobile robot can be added with more ultrasonic sensors to detect the object because some of the object cannot be detected if only one sensor used in mobile robot. Another sensor also can be used such as laser range finder to detect the surrounding environment. Besides, the path planning and path following algorithms can apply in this system. The path planning algorithm to give the mobile robot can traverse through to reach a target destination while the path following algorithms to allow the robot to move to a target point. This will make mobile robot move freely in indoor environment. Other than that, simultaneous localization and mapping (SLAM) algorithms can used as a means to localize and map surrounding area for mobile robot.

REFERENCES

This thesis is prepared based on the following references;

Ali, W. G. (2011). A semi-autonomous mobile robot for education and research. *Journal of King Saud University - Engineering Sciences*, *23*(2), 131–138. https://doi.org/10.1016/j.jksues.2011.03.007

Araújo, A., Couceiro, M. S., & Rocha, R. P. (2013). Integrating Arduino - based Educational Mobile Robots in ROS. *13th International Conference on Autonomous Robot Systems*, 9–14. https://doi.org/10.1109/Robotica.2013.6623520

Becerra, H. M., Courbon, J., Mezouar, Y., & Sagues, C. (2010). Wheeled mobile robots navigation from a visual memory using wide field of view cameras. *2010 IEEE/RSJ International Conference on Intelligent Robots and Systems*, 5693–5699. https://doi.org/10.1109/IROS.2010.5650114

CERKALA, J., & JADLOVSKÁ, A. (2015). Nonholonomic Mobile Robot With Differential Chassis Mathematical Modelling and Implementation in Simulink With Friction in Dynamics. *Acta Electrotechnica et Informatica*, *15*(3), 3–8. https://doi.org/10.15546/aeei-2015-0021

Goris, K. (2005). Autonomous mobile robot mechanical design. *Verije University, Brussels*. Retrieved from http://mech.vub.ac.be/multibody/final_works/ThesisKristofGoris.pdf

Hatab, A. A., & Dhaouadi, R. (2013). Dynamic Modelling of Differential-Drive Mobile Robots using Lagrange and Newton-Euler Methodologies: A Unified Framework. *Advances in Robotics & Automation*, *2*(2). https://doi.org/10.4172/2168-9695.1000107

Kim, Y., Kim, S. H., & Kwak, Y. K. (2005). Dynamic analysis of a nonholonomic two-wheeled inverted pendulum robot. *Journal of Intelligent and Robotic Systems: Theory and Applications*, *44*(1), 25–46. https://doi.org/10.1007/s10846-005-9022-4

Klančar, G., Matko, D., & Blai, S. (2011). A control strategy for platoons of differential drive wheeled mobile robot. *Robotics and Autonomous Systems*, *59*(2), 57–64. https://doi.org/10.1016/j.robot.2010.12.002

Lee, S., Oh, S., & Korea, S. (2014). m Onl ad in e b e V y er th si is on fil O e i n s I ly . Bo m Onl ad in e b e V y er th si is on fil O e i n s I ly ., *7*(3), 113–124.

Mak. (2015). Realization of Mini Segway Robot Using NI MyRIO, (February).

Malu, S. K., & Majumdar, J. (2014). Kinematics, Localization and Control of Differential Drive Mobile Robot. *Global Journal of Researches in Engineering*, *14*(1), 1–8.

Meghdari, A. (2004). Dynamics modeling of "cedra" rescue robot on uneven terrains.

Asme 2004 ..., *13*(3), 272–283. https://doi.org/10.1115/IMECE2004-59239

Mester, G. (2006). Motion Control of Wheeled Mobile Robots Modeling of the Wheeled Mobile Robots. *4th Serbian-Hungarian Joint Symposium on Intelligent Systems, SISY*, 119–130.

Rajan, C., Megala, B., Nandhini, A., & Priya, C. R. (2015). A Review : Comparative Analysis of Arduino Micro Controllers in Robotic Car, *9*(2), 371–380.

Ribeiro, F., Moutinho, I., Silva, P., Fraga, C., & Pereira, N. (2004). Three Omni-Directional Wheels Control on a Mobile Robot. *Control 2004*.

Sabto, N. A., & Mutib, K. Al. (2013). Autonomous mobile robot localization based on RSSI measurements using an RFID sensor and neural network BPANN. *Journal of King Saud University - Computer and Information Sciences*, *25*(2), 137–143. https://doi.org/10.1016/j.jksuci.2012.10.001

Shamrao, P. S., & Awale, R. N. (2016). Simulation of nonlinear filter based localization for indoor mobile robot, *4*(5), 183–184. https://doi.org/10.17148/IJIREEICE.2016.4546

Shamsudin, M. A., Mamat, R., & Nawawi, S. W. (2013). Dynamic Modelling and Optimal COntrol Scheme of Wheel Inverted Pendulum for Mobile Robot Application, *3*(6), 1–20.

Sharma, K. (2015). Kinect Sensor based Object Feature Estimation in Depth Images, *8*(12), 237–246.

Shojaei, K., Mohammad Shahri, A., & Tarakameh, A. (2011). Adaptive feedback linearizing control of nonholonomic wheeled mobile robots in presence of parametric and nonparametric uncertainties. *Robotics and Computer-Integrated Manufacturing*, *27*(1), 194–204. https://doi.org/10.1016/j.rcim.2010.07.007

SinghPannu, G., Dawud Ansari, M., & Gupta, P. (2015). Design and Implementation of Autonomous Car using Raspberry Pi. *International Journal of Computer Applications*, *113*(9), 22–29. https://doi.org/10.5120/19854-1789

Song, L., Fei, Y., & Lu, T. (2009). Study on effects of nonholonomic constraints on dynamics of a new developed quadruped leg-wheeled passive mobile robot. *WSEAS Transactions on Systems*, *8*(1), 137–147.

Tölgyessy, M., & Hubinský, P. (2010). The Kinect Sensor in Robotics Education. *International Conference on Robotics in Education*, (November), 143–146.

Ujjainiya, L., & Chakravarthi, M. K. (2015). Raspberry – Pi Based Cost Effective Vehicle Collision Avoidance System Using Image Processing. *ARPN Journal of Engineering and Applied Scieces*, *10*(7), 3001–3005.

Warade, S., Aghav, J., Petitpierre, C., & Udayagiri, S. (2012). Automated Training and Maintenance through KINECT. *International Journal of Computer Science, Engineering and Applications*, *2*(3), 159–172. https://doi.org/10.5121/ijcsea.2012.2315

White, W. N., Wagner, J., Blankenau, B., Wang, Z., & Salazar, V. (2015). Design , Build , and Test of an Autonomous Inverted Pendulum Cart. *The American Control Conference*, 2783–2788.

APPENDIX A
GANTT CHART

Month	Setpember				October			November				December			January		February				March				April			
Activities/Week	1	2	3	4	5	6	7	8	9	10	11	12	13	14	1	2	3	4	5	6	7	8	9	10	11	12	13	14
Literature Review	■	■	■	■	■																							
Study and Learn about Kinect and myRIO						■	■	■	■																			
Study and Learn for LabVIEW										■	■	■																
Integrate Algorithum to myRIO and Kinect													■	■														
Develop Prototype Mobile Robot															■	■												
Integarate the Hardware to Mobile Robot																	■	■										
Test Run for Mobile Robot																			■	■								
Robot Finalization																					■	■	■					
Report Writing																								■	■	■		
Final Paper Review and Submission																											■	■

APPENDIX B
LABVIEW SIMULATION FOR WMR

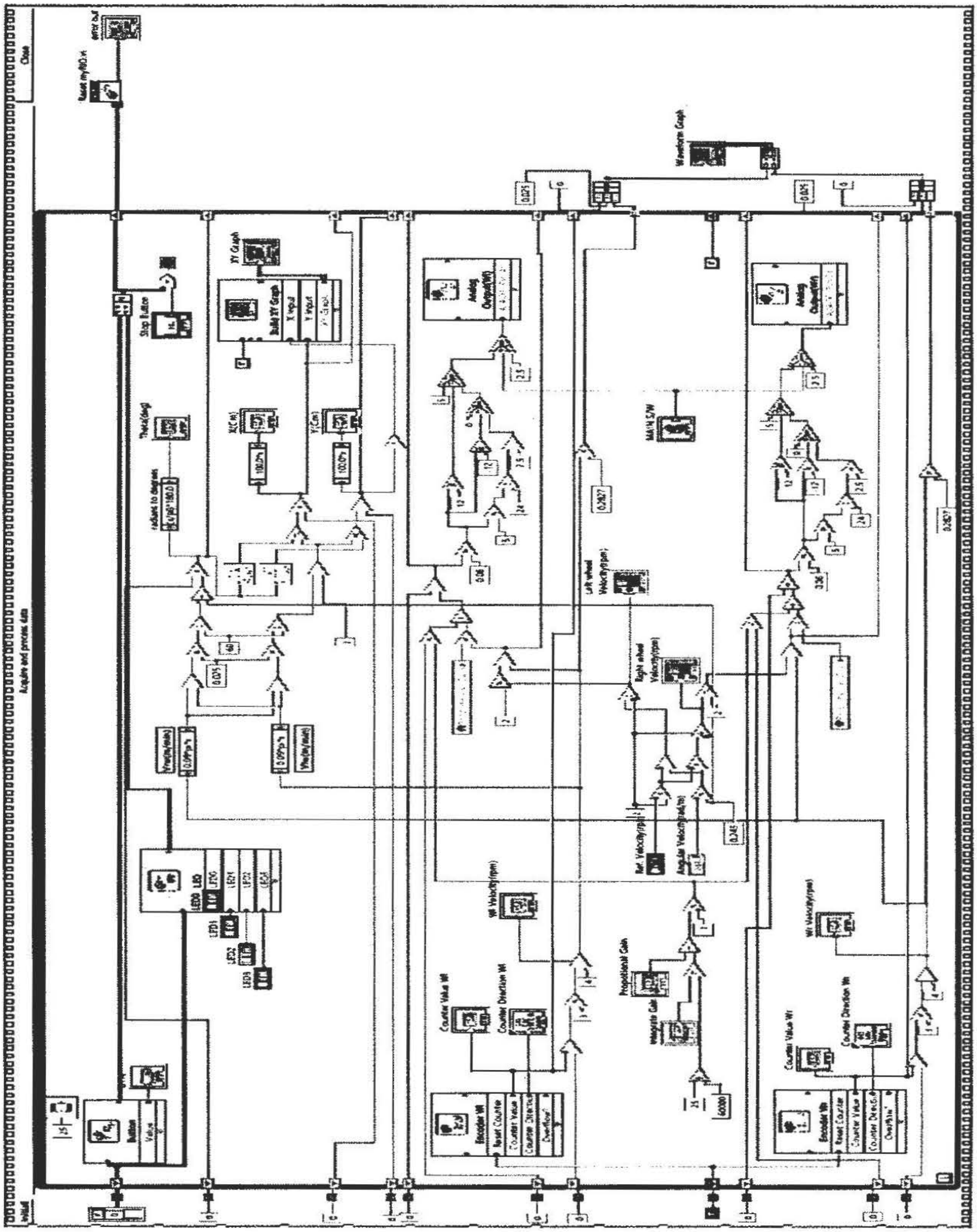

APPENDIX C
LABVIEW SIMULATION FOR ULTRASONIC SENSOR

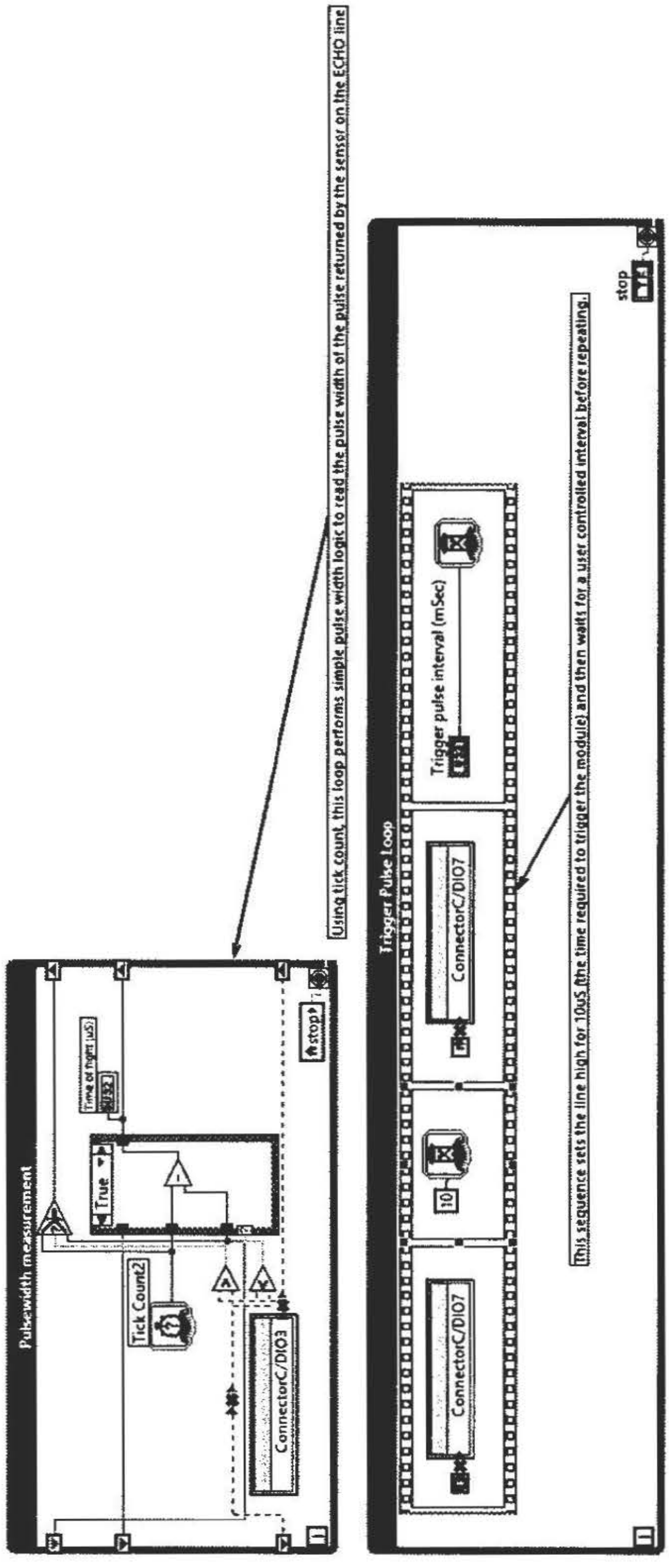

APPENDIX D
LABVIEW SIMULATION FOR KINECT SENSOR

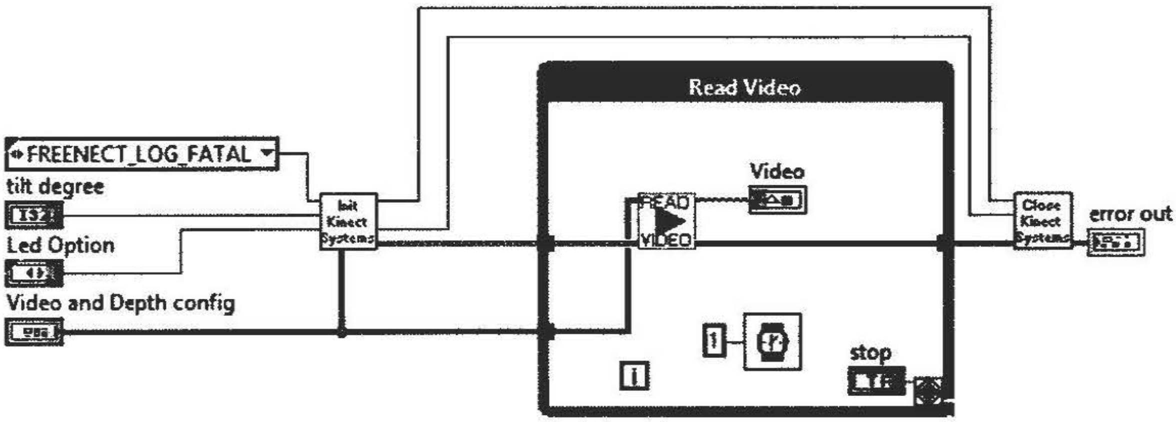

APPENDIX E
CONFERENCE PAPER

Autonomous Mobile Robot Using MyRIO

YONG ZONG WEI
Bachelor in Mechatronics Engineering,
Faculty of Manufacturing Engineering, Universiti Malaysia Pahang (UMP), Kampus Pekan, 26600 Pekan, Pahang, Malaysia.

Abstract

The research study is conducted to develop an autonomous mobile robot algorithm with implementation of dynamic modelling using Newton-Euler approach.The rigid body of the mobile robot is equipped with two wheels and a castor for the purpose of simple control and stable balancing. In addition, Kinect motion sensor will be applied for the image detection and video recording while ultrasonic sensor obstacle avoidance of the mobile robot. On the other hand, the simulation of the control mechanism is realized through LabVIEW software package where the development of the mobile robot environment is carried out and transferred to National Instrument myRIO hardware.

***Keyword**: Autonomous mobile robot, Dynamic modelling, Kinect sensor, Ultrasonic sensor, LabVIEW, myRIO*

INTRODUCTION

Robotics had subdivided off the science that includes electrical engineering, manufacturing engineering, mechatronics engineering and others. As we know, robotics had attained a greatest successful in industrials on this world. There are many types of industrial applications using robotics such as the robot arm, mobile robots and other. The most popular robotics on this world is mobile robots. The hardware and software of mobile robot has been designed for the purpose of extreme environment, such that it will be able to perform their tasks in the presence of noise. In some cases where dynamic environment is involved, the mobile robot could not be able to perform good task such that the feedback from the robot is contradictory to the current situation being measured and inconsistent response information for a continuously changing environment. (Ali, 2011). Nowadays, mobile robots have been evolving to move automatically from one places to other locations. For daily activities, mobile robots have been extensively developed and researched to assist humans for doing daily activities. Mobile robots is widely developed to reduce human work and easy the job. In this situation, mobile robots can expand work to convey an expanding inclination for mechanical fabricating exercise. Typically, the above-described mobile robots will used in industrials.

However, due to extensive research in mobile robot. There are a lot of application of mobile robots for nowadays. Every situation in which an animal, human or vehicle involves in a useful work today provides a potential application for a mobile robot. Based on reports, by implementing mobile robot in industrial manufactures can improve product quality, reduce overheads, increase rates of production and so on. Mobile robots types and application will show at the figure below.

The widely used type of mobile robots are wheeled mobile robot also can name as WMR. WMR are most popular in mobile robots because WMR uses differential-drive system and it is also alternative for the purpose of simple design and manoeuvrable. Simple explanation for WMR are combination with computational (software) and various physical (hardware) components. Simple implementations of WMR subsystem are locomotion, sensing, communication, reasoning and control. Each subsystems will apply in WMR.

WMR does not only depend on the tracking system, the control and drive system also necessary. For the control algorithm, it made up with the mathematical model properties in WMR. The mathematical model for WMR can explain in two ways, which are dynamics and kinematic models. Commonly dynamic modelling will be omitted when developing in mathematical models of WMR (Shojaei et al., 2011). While both modelling are the preferred system accuracy.

Apart from that, navigation mobile robots also famous and widely in the field of robotics.

Navigation can be combination of the self – localisation, path planning and map-building competence (Becerra et al., 2010). National Instruments myRIO (NI myRIO) is an embedded hardware device to proven technology and allows to design real, complex engineering systems more quickly and affordably than ever before. NI myRIO can incorporate the interfacing and advantages for programming in LabVIEW (White et al., 2015).

In this project, the mobile robot is considered as autonomous, if it has a few capabilities. Mobile robot should be able to locate at indoor environment. Lastly, mobile robot should be detect navigate an environment with obstacles while using ultrasonic and Kinect sensor as image capture.

PROBLEM STATEMENT

Nowadays, service application for autonomous mobile robot have been considered such as intelligent wheelchair, food delivery and vacuum cleaners mobile robot. For those robots, it must recognize a specific object and it can be required to relocate and approach. The navigation can used in a mobile robot to develop a control system. An optimal navigation system that enables he mobile robot to move in entire area. The choice of vision based object recognition technique for mobile robot have some difficult such as direct the mobile robot to move and relocate as required that will involves selecting vision sensor's viewpoint. The most challenging problem is the object detection process because mobile robot need to navigate and place the object in view field. Besides that, the mobile robot also required a vision system that can use in image analysis techniques to environmental conditions like background colour.

OBJECTIVE

The objectives of this project are as below:

1. To design a robot with mobility in indoor environment.
2. To accomplish object avoidance using ultrasonic sensor while Kinect sensor as image capture.
3. To develop LabVIEW simulation for the robot's control.

METHODOLOGY

Project Flow Chart

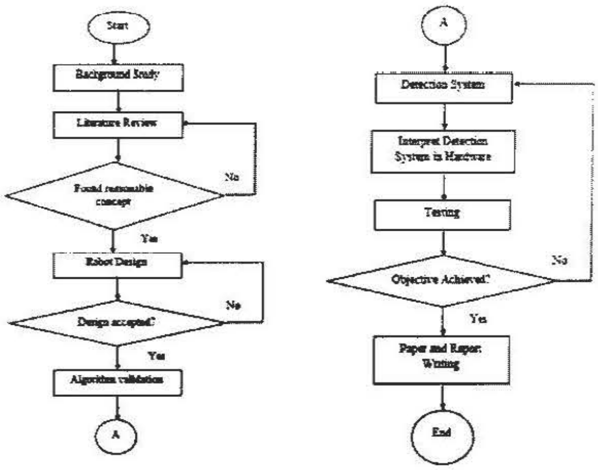

Figure 1: Project flow chart

PID Theory

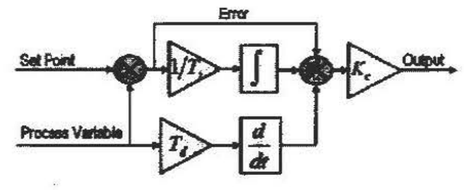

Figure 2: Block diagram for a basic PID control alogrithum

The proportional term can produces an output value that proportinal to the current error value. The proportional gain constant, K_p as the proportional response can be adjusted by multiplying the error with constant K_p.

$$P_{out} = K_p e(t)$$

The integral term is proportional to both the magnitude of error and duration of the error. The accumulated error is then multiplied by the integral gain, K_i and added to the controller output.

$$I_{out} = K_i \int_0^t e(\tau)d\tau$$

The derivative of the process error is calculated by determining the slope of the error over time and multiplying this rate of the change by the derivative gain, K_d Derivative gain, K_d is a magnitude of the contribution of the derivative term to overall control action

$$D_{out} = K_d \frac{de(t)}{dt}$$

The PID controller algorithm can show as below:

$$u(t) = MV(t) = K_p e(t) + K_i \int_0^t e(\tau)d\tau + K_d \frac{de(t)}{dt}$$

Model Development

There are two types of modelling involved in autonomous mobile robot. The first is the kinematic model of the mobile robot which is influences the differential drive system of the robot. After the kinematic model, the dynamic modelling of the autonomous mobile robot which will includes the electro-mechanical system.

Kinematics Model

The differential drive model is derived from the forward kinematics equation. It represent elementary model where all physical issues like inertia, friction and mechanical structure inaccuracy are neglected.

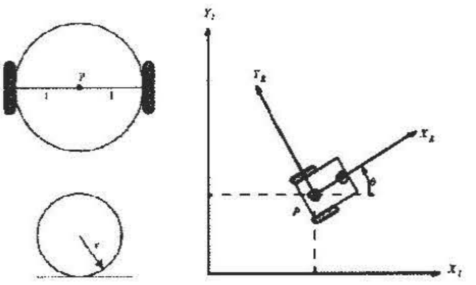

Figure 3: Forward Kinematic model and robot position frames

Define the robot motion as below:

$$\dot{\xi}_I = \begin{bmatrix} \dot{x} \\ \dot{y} \\ \dot{\theta} \end{bmatrix} = g(l, r, \theta, \omega_1, \omega_2)$$

$$R(\theta) = \begin{pmatrix} \cos(\theta) & \sin(\theta) & 0 \\ -\sin(\theta) & \cos(\theta) & 0 \\ 0 & 0 & 1 \end{pmatrix}$$ Thus,

describing the motion of the robot between the frames $\dot{\xi}_R = R(\theta)\dot{\xi}_I$

$$\therefore \dot{\xi}_I = R(\theta)^{-1}\dot{\xi}_R$$

Considering a simple 90° point turn where $\theta = \pi/2$ and substitute into above:

$$\therefore \dot{\xi}_R = R\left(\frac{\pi}{2}\right)\dot{\xi}_I = \begin{bmatrix} 0 & 1 & 0 \\ -1 & 0 & 0 \\ 0 & 0 & 1 \end{bmatrix} \begin{bmatrix} \dot{x} \\ \dot{y} \\ \dot{\theta} \end{bmatrix} = \begin{bmatrix} \dot{y} \\ -\dot{x} \\ \dot{\theta} \end{bmatrix}$$

Inverting the standard orthogonal rotational transformation for equation above,

$$R(\theta)^{-1} = \begin{bmatrix} \cos(\theta) & -\sin(\theta) & 0 \\ \sin(\theta) & \cos(\theta) & 0 \\ 0 & 0 & 1 \end{bmatrix}$$

The model at figure 3, the speed of each wheel is $r\omega$ and hence the translational speed is given by the average velocity:

$$\dot{x}_R = r\left(\frac{\omega_1 + \omega_2}{2}\right)$$

Instantaneous rotation P for one wheel:

$$\omega_1 = r\frac{\omega_1}{2l}$$

The complete rotation:

$$\dot{\theta} = \frac{r}{2l}(\omega_1 - \omega_2)$$

Substituting equation all equation to obtain the differential drive model:

$$\dot{\xi}_I = \begin{bmatrix} \cos(\theta) & -\sin(\theta) & 0 \\ \sin(\theta) & \cos(\theta) & 0 \\ 0 & 0 & 1 \end{bmatrix} \frac{r}{2} \begin{bmatrix} \omega_1 + \omega_2 \\ 0 \\ \dfrac{\omega_1 - \omega_2}{l} \end{bmatrix} = \begin{bmatrix} \dot{x} \\ \dot{y} \\ \dot{\theta} \end{bmatrix}$$

Dynamic Model

The dynamic model developed was based on Newton-Euler approach. For this model, it consists of dynamic behaviour of the robot chassis and DC motors. The model derived is based on centre of mass dynamics. Besides that, this model extends standard model by including the dynamic part describing dependency of wheel speed and motor supply voltage. Moreover, the dynamics, construction, geometry and other parameters of chassis and motor were included.

The model was an adaptation from F. Dušek (2011) and the parameters were modified to the model WMR that is developed. The work is started by taking force balance for the derivation of motion equation.

$$\overline{F} + \underbrace{\left(m\frac{d\bar{v}}{dt}\right)}_{\substack{\text{Inertial}\\ \text{force}}} + \underbrace{\left(m\frac{d\bar{\omega}}{dt} \times r\right)}_{\substack{\text{Euler's}\\ \text{force}}} + \underbrace{\left(2m\bar{\omega} \times \frac{d\bar{r}}{dt}\right)}_{\substack{\text{Coriolis}\\ \text{force}}} + \underbrace{\left[m\bar{\omega} \times \left(\bar{\omega} \times \bar{r}\right)\right]}_{\substack{\text{Centrifugal}\\ \text{force}}} = 0$$

Development Overall model and steady-state come out with four differential equations describing the behaviour of both engines as figure 4.

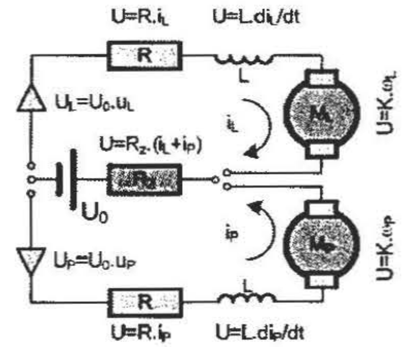

Figure 4: Two DC motors wiring

$$Ri_L + R_Z(i_L + i_P) + L\frac{di_L}{dt} = u_L U_0 - K\omega_L$$

$$Ri_p + R_Z(i_L + i_P) + L\frac{di_P}{dt} = u_P U_0 - K\omega_P$$

$$J\frac{d\omega_L}{dt} + k_r\omega_L + M_L = Ki_L \quad , \quad J\frac{d\omega_P}{dt} + k_r\omega_P + M_P = Ki_p$$

The reduced wheel radius r_G and total moment of inertia J_B as shown in equation as below.

$$r_G = \frac{r}{p_G}; \quad J_B = J_T + ml_T^2$$

$$\frac{p_G}{r}M_L + \frac{p_G}{r}M_P - k_v v_B - m\frac{dv_B}{dt} = 0$$

$$M_L + M_p - r_G k_v v_B - r_G m\frac{dv_B}{dt} = 0$$

$$-l_L\frac{p_G}{r}M_L + l_P\frac{p_G}{r}M_P - k_\omega\omega_B - (J_T + ml_T^2)\frac{d\omega_B}{dt} = 0$$

$$-l_L M_L + l_P M_P - k_\omega\omega_B - r_G J_B\frac{d\omega_B}{dt} = 0$$

$$v_B = \frac{r_G}{l_L + l_P}(l_P\omega_L + l_L\omega_P) \quad , \quad \omega_B = \frac{r_G}{l_L + l_P}(-\omega_L + \omega_P)$$

To derive the steady-state since the equations are linear with respect to state variables. The steady-state is represented in matrix form as shown in equation below.

$$\begin{bmatrix} R+R_z & R_z & K & 0 & 0 & 0 & 0 & 0 \\ R_z & R+R_z & 0 & K & 0 & 0 & 0 & 0 \\ K & 0 & -k_r & 0 & -1 & 0 & 0 & 0 \\ 0 & K & 0 & -k_r & 0 & -1 & 0 & 0 \\ 0 & 0 & 0 & 0 & 1 & 1 & -r_G k_v & 0 \\ 0 & 0 & 0 & 0 & -l_L & l_P & 0 & -r_G k_\omega \\ 0 & 0 & l_P & l_L & 0 & 0 & -\frac{l_P + l_L}{r_G} & 0 \\ 0 & 0 & -1 & 1 & 0 & 0 & 0 & -\frac{l_P + l_L}{r_G} \end{bmatrix} \begin{bmatrix} i_L \\ i_P \\ \omega_L \\ \omega_P \\ M_L \\ M_P \\ v_B \\ \omega_B \end{bmatrix} = \begin{bmatrix} U_L \\ U_P \\ 0 \\ 0 \\ 0 \\ 0 \\ 0 \\ 0 \end{bmatrix}$$

The linear part of the model can be modified into simpler form equation,

$$a_L = k_r + \frac{k_v l_P r_G^2}{l_L + l_P}; \quad a_P = k_r + \frac{k_v l_L r_G^2}{l_L + l_P}$$

$$b_L = J + \frac{ml_P r_G^2}{l_L + l_P}; \quad b_P = J + \frac{ml_L r_G^2}{l_L + l_P}$$

$$c_L = k_r l_L + \frac{k_\omega r_G^2}{l_L + l_P}; \quad c_P = k_r l_P + \frac{k_\omega r_G^2}{l_L + l_P}$$

$$d_L = Jl_L + \frac{J_B r_G^2}{l_L + l_P}; \quad d_P = J_P + \frac{J_B r_G^2}{l_L + l_P}$$

The reduce linear part of the model equations shown as below

$$\frac{di_L}{dt} = \frac{u_L U_0 - K.\omega_L - (R + R_Z).i_L - R_Z i_P}{L}$$

$$\frac{di_P}{dt} = \frac{u_P U_0 - K.\omega_P - (R + R_Z).i_P - R_Z i_L}{L}$$

$$\frac{d\omega_L}{dt} = \frac{1}{b_L d_P + b_P d_L}\begin{pmatrix} d_P\left[K\left(i_L + i_P\right) - a_L\omega_L - a_P\omega_P\right] \\ -b_P\left[K\left(-l_L i_L + l_P i_P\right) + c_L\omega_L - c_P\omega_P\right] \end{pmatrix}$$

$$\frac{d\omega_P}{dt} = \frac{1}{b_L d_P + b_P d_L}\begin{pmatrix} d_L\left[K\left(i_L + i_P\right) - a_L\omega_L - a_P\omega_P\right] \\ +b_L\left[K\left(-l_L i_L + l_P i_P\right) + c_L\omega_L - c_P\omega_P\right] \end{pmatrix}$$

The reduced linear part is presented in standard state-space model in matrix from as shown in equation below.

$$\frac{dx}{dt} = Ax + Bu$$
$$y = Cx$$
$$where$$
$$x = \begin{bmatrix} i_L \\ i_P \\ \omega_L \\ \omega_P \end{bmatrix} \quad u = \begin{bmatrix} u_L \\ u_P \end{bmatrix} \quad y = \begin{bmatrix} v_B \\ \omega_B \end{bmatrix}$$

Constant matrices A, B and C will show as below

$$A = \begin{bmatrix} -\frac{R+R_Z}{L} & -\frac{R_Z}{L} & -\frac{K}{L} & 0 \\ -\frac{R_Z}{L} & -\frac{R+R_Z}{L} & 0 & -\frac{K}{L} \\ \frac{K(d_P+b_P l_L)}{b_L d_P + b_P d_L} & \frac{K(d_P-b_P l_P)}{b_L d_P + b_P d_L} & -\frac{d_P a_L + b_P c_L}{b_L d_P + b_P d_L} & -\frac{d_P a_P - b_P c_P}{b_L d_P + b_P d_L} \\ \frac{K(d_L-b_L l_L)}{b_L d_P + b_P d_L} & \frac{K(d_L+b_L l_P)}{b_L d_P + b_P d_L} & -\frac{d_L a_L - b_L c_L}{b_L d_P + b_P d_L} & -\frac{d_L a_P + b_L c_P}{b_L d_P + b_P d_L} \end{bmatrix}$$

$$B = \begin{bmatrix} \frac{U_0}{L} & 0 \\ 0 & \frac{U_0}{L} \\ 0 & 0 \\ 0 & 0 \end{bmatrix}$$

$$C = \begin{bmatrix} 0 & 0 & \frac{l_P r_G}{l_L + l_P} & \frac{l_L r_G}{l_L + l_P} \\ 0 & 0 & -\frac{r_G}{l_L + l_P} & \frac{r_G}{l_L + l_P} \end{bmatrix}$$

Kinect Data Processing For Capture Image

There are three resolutions supported by the depth stream are 640 x 480 pixels, 320 x 240 pixels, and 80 x 60 pixels. The depth data contains the distance information to the nearest object from the camera plane at a particular (*x*, *y*) coordinate. Besides that, depth sensor's field of view range remains the same as the field of view of color camera. an IR emitter and An IR depth sensor that is a monochrome CMOS (Complementary Metal-Oxide-Semiconductor) sensor to capture the 3D information of an object for the Kinect sensors. Depth data processing are detailed will show as below figure 5.

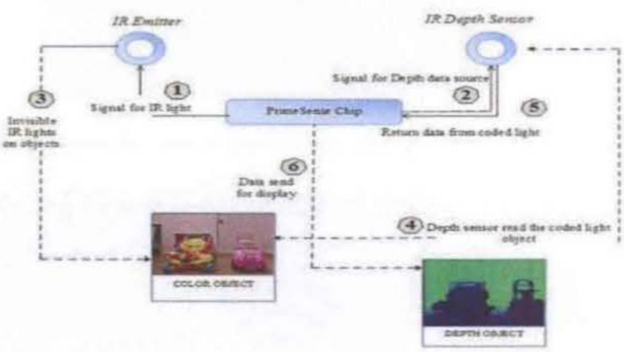

Figure 5: Data processing for Kinect

LabVIEW Simulation

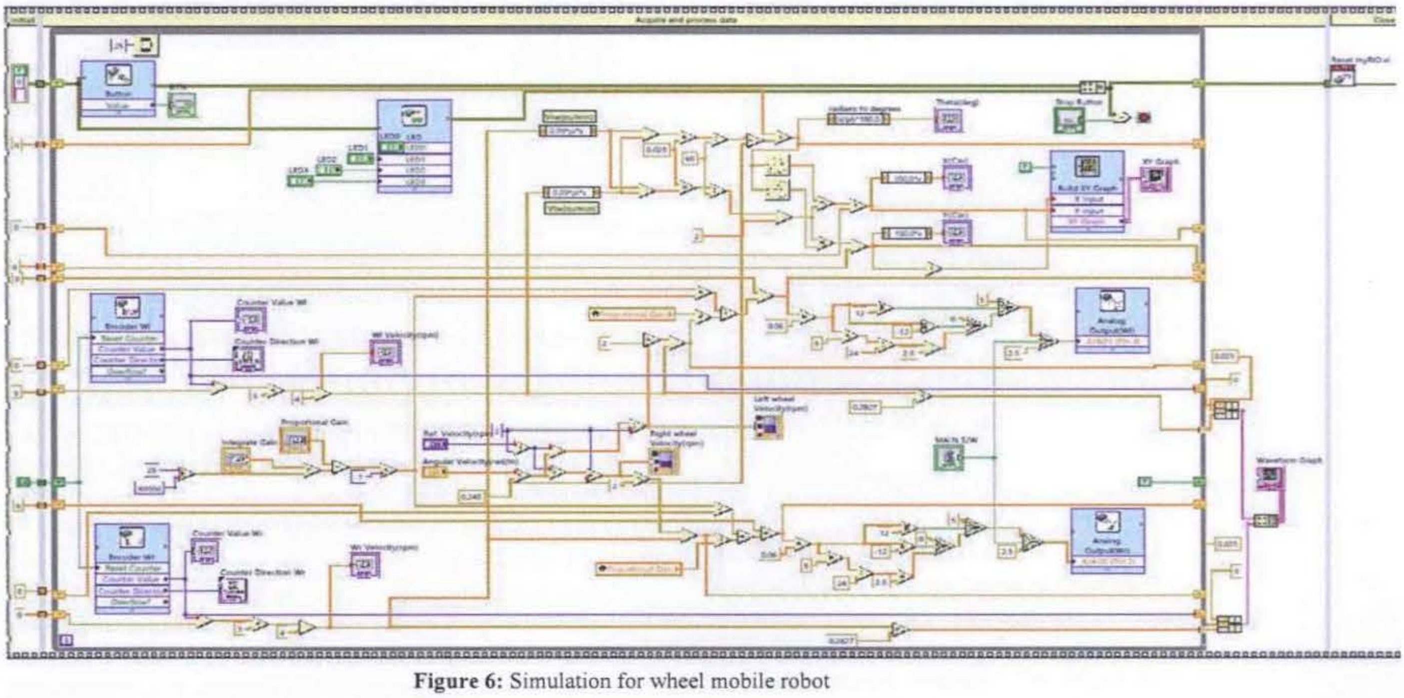

Figure 6: Simulation for wheel mobile robot

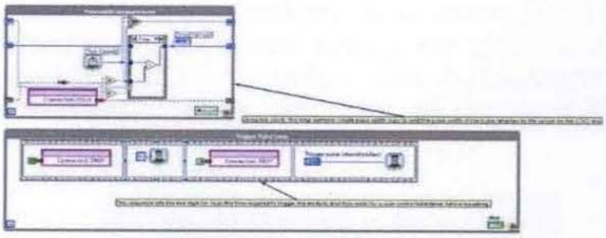

Figure 7: Simulation for ultrasonic sensor

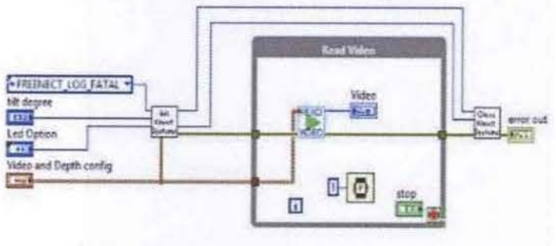

Figure 8: Simulation for Kinect sensor

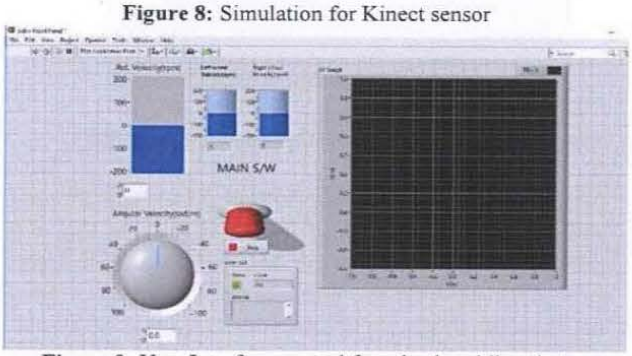

Figure 9: User Interface control for wheel mobile robot

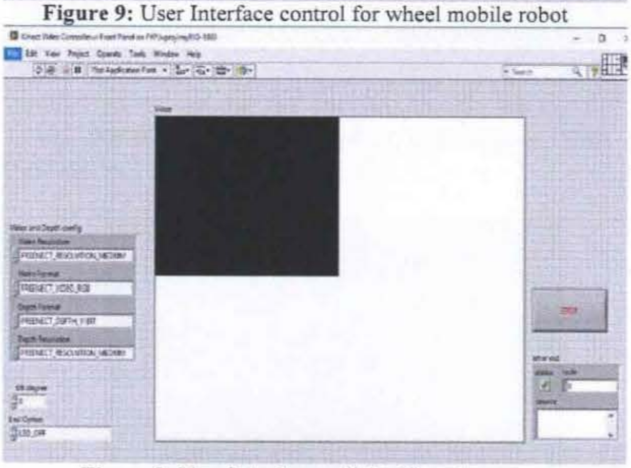

Figure 8: User Interface wall for Kinect sensor

The simulation at the LabVIEW as shown in Figure 6, 7 and 8. The block diagram arranged and the simulation was conducted. While the calculation and the PID control that using in WMR as shown in figure 6. In Figure 6 the quadrature encoder have used to provide closed loop feedback for position and velocity controlled applications at motor driver control system. While using quadrature encoder for velocity and acceleration control in high speed and precision applications, it can process quadrature encoder signals (velocity, acceleration and instantaneously output controls signals) at hardware timed precision. Figure 9 is the user interface wall in LabVIEW simulation for PWM signals in rpm and observe the motor response. Figure 10 is Kinect sensor will start to capture or video when run the simulation and shown in the user interface wall.

Overall Hardware Structure

The mechanical and equipment with all electrical part of the mobile robot have been assembled and the final output as shown in figure 11

Figure 11: Overall hardware for mobile robot

Working Principle of the Mobile Robot

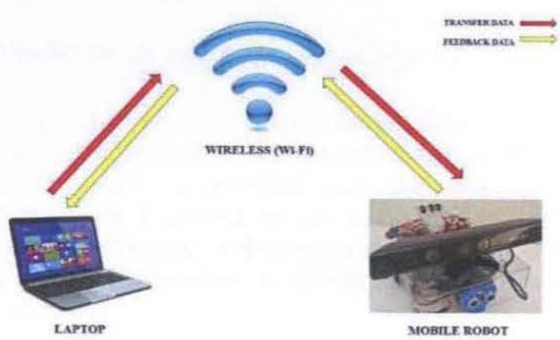

Figure 12: Flow of the system

The LabVIEW simulation have been done at laptop and using the Wi-Fi system to transfer the data for myRIO. The myRIO will receives the data and process it. The mobile robot will start moving and the Kinect sensor will start to record video while the ultrasonic will obstacle the object. The video that have record will send feedback to the user interface wall at the LabVIEW simulation.

RESULTS

LabVIEW result for WMR

The software used for simulation is done in LabVIEW 2013. The result of simulation will be discussed later in this chapter. The block diagram are made in LabVIEW for getting the image and depth data from Kinect then transfer the simulation to myRIO. The simulated system will tested out the data on WMR. The simulation results taken when the myRIO connect with the motor drivers WMR. When the motor drivers turning, the results will show in the user interface wall in LabVIEW simulation. There are three results in this simulation shown in figure 13, 14 and 15.

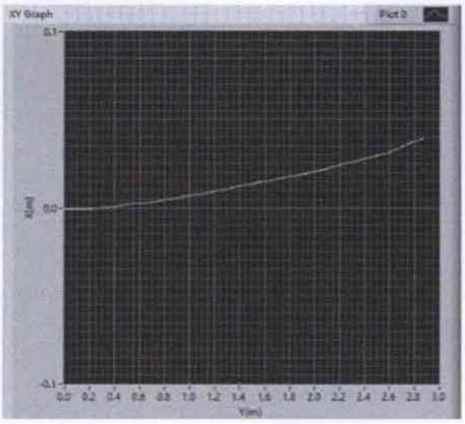

Figure 13: WMR motion respect to X and Y coordinate

Base on figure 13, the first user interface wall shows the left and right wheel in constant velocity (100 rpm). The speed of the wheels remain constant as long as the velocity is same for both wheels. The WMR will move in linearly position. Figure 13 shows that WMR motion respect to X and Y coordinate. Normally, X and Y should be constant when take the result. But the graph at X-axis is small increasing due to the initial slip when the motor starts running. Therefore the mobile robot head to left in small angle.

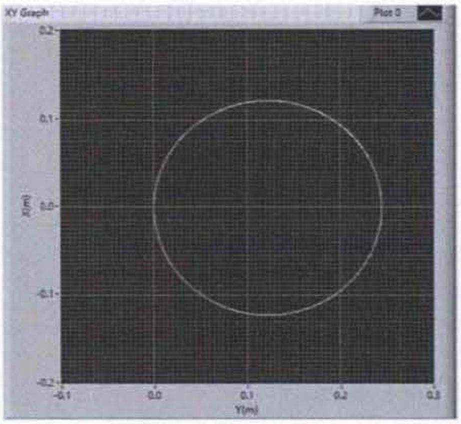

Figure 14: WMR motion respect to X and Y coordinate

While on the figure 14, is used the angular velocity is 7 rad/m that calculate by using the equation above. The left wheel velocity is 50 rpm but right wheel velocity is 100 rpm and cause the right wheel move faster speed than the left wheel. In this situation, create a motion toward to left side. Other than that, the X and Y coordinates shown a circular motion in left direction that shown in figure 14. As a result, the mobile robot is moving towards left and become circular pattern.

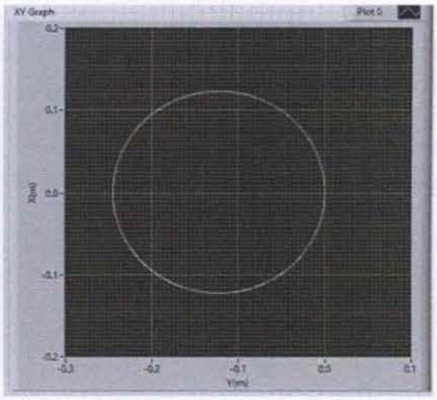

Figure 15: WMR motion respect to X and Y coordinate

In figure 15, is used the angular velocity is -7 rad/m. The left wheel velocity is 100 rpm but right wheel velocity is 50 rpm and cause the left wheel move faster speed than the right wheel. This cause the right wheel will slow and left wheel turn to right side. Furthermore, in figure 15 the X and Y coordinates shown a circular motion in right direction. As a result, the mobile robot is moving towards right and become circular pattern.

LabVIEW result for ultrasonic sensor

Thought this simulation, the ultrasonic sensor can obstacle the distance between the object and mobile robot. In order to generate the ultrasonic in simulation, the Trig need to set at high state for 10μs and Echo output will in microseconds sound wave traveled. Therefore, to obtain the time taken between the object and mobile robot, there are some results that taken from simulation and using the mathematic calculation to get time taken that needed. Table 1 will show the results in Echo (μs) by ultrasonic sensor.

Table 1: Echo (μs) results

No	Time taken (μs)	Distance (cm)
1.	1764	30
2.	1470	25
3.	1176	20
4.	882	15

Mathematic formula to calculate the distance is time taken (μs) multiple by speed of sound (340 m/s or 0.034 cm/ μs) and divided by 2 because sound wave need to travel forward and backward to detect the distance. Asa a result, mobile robot stop at 20 cm after get the time taken that need for stop when obstacle the object.

LabVIEW result for Kinect sensor

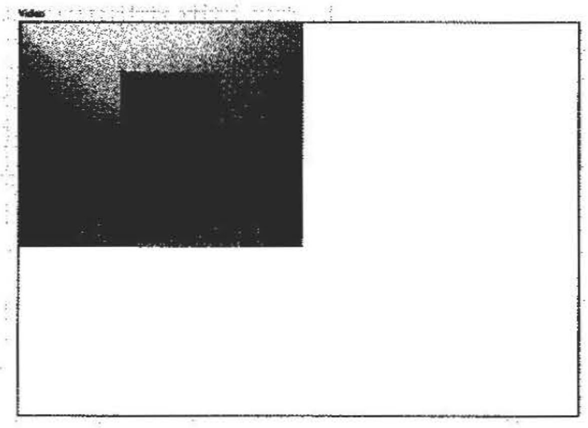

Figure 16: Part of video record when mobile robot moving

Table 2: Experimental parameter used

Parameters	Value
Data Stream	Color
Resolution	640 x 480 pixels (medium) Color image
Components used in Kinect sensor	Color camera, IR emitter and IR depth sensor
LED	If LED turns green, Kinect device drivers installed properly
Tilt motor	Tilted vertically can upwards or downwards by 27 degrees of the motor

USB Kinect sensor must connect to myRIO, but before that, library for Kinect sensor must install in myRIO. The library are based on the model 1414 Kinect sensor. Kinect sensor will start to capture or video when run the simulation. The user interface wall for Kinect sensor will show at above figure. While video and image capture shown in figure 16. Table 2 shown experimental parameter used.

CONCLUSION

Overall for this research, the autonomous mobile robot using myRIO have been discussed. The kinematic and dynamic equations have been discussed and derived base on the previous studies and research. Both equations were used in WMR mobile robot and apply in the LabVIEW simulation. The results were successfully while apply the both equations. PID controller have been used in LabVIEW simulation and successfully to give mobile robot moving in constant speed. Besides, the Kinect sensor and ultrasonic sensor in LabVIEW simulation have been successful apply in mobile robot through myRIO hardware. The autonomous mobile robot hardware have successfully install with all components that haven been mention before and work while taken the experiments.

To conclude, autonomous mobile robot have been successfully developed. The experiment results have been successfully but when LabVIEW simulation compare with the both equations have difference because real hardware will more accurate compare with the equation. While the equations also very important while design a mobile robot to know how it apply and working principle. However, when doing LabVIEW simulation, most challenge was the LabVIEW system because LabVIEW have a lot of block diagram and special icon. The time for research LabVIEW was used a lot and understand it. Moreover, used Wi-Fi to transfer data was no stable compare using USB from computer. The data will delay when using Wi-Fi and the mobile robot will delay. In a whole, the mobile robot was successful capture image, record video and obstacle object.

ACKNOWLEDGEMENT

The authors would like to express gratitude and acknowledge the Facility of Manufacturing Engineering, Universiti Malaysia Pahang (UMP) for continuous support

REFERENCES

1. Ali, W. G. (2011). A semi-autonomous mobile robot for education and research. *Journal of King Saud University - Engineering Sciences*, *23*(2), 131–138. https://doi.org/10.1016/j.jksues.2011.03.007
2. Araújo, A., Couceiro, M. S., & Rocha, R. P. (2013). Integrating Arduino - based Educational Mobile Robots in ROS. *13th International Conference on Autonomous Robot Systems*, 9–14. https://doi.org/10.1109/Robotica.2013.6623520